

UNITED STATES  
DEPARTMENT OF THE INTERIOR  
GEOLOGICAL SURVEY

TWO-DIMENSIONAL, STEADY-STATE MODEL OF GROUND-WATER FLOW,  
NEVADA TEST SITE AND VICINITY, NEVADA-CALIFORNIA  
By Richard K. Waddell

---

U.S. GEOLOGICAL SURVEY  
WATER RESOURCES INVESTIGATIONS 82-4085

Prepared in cooperation with the  
U.S. DEPARTMENT OF ENERGY

Denver, Colorado  
1982

UNITED STATES DEPARTMENT OF THE INTERIOR

JAMES G. WATT, Secretary

GEOLOGICAL SURVEY

Dallas L. Peck, Director

---

For additional information  
write to:

Water Resources Division, Central Region  
U.S. Geological Survey  
Box 25046, Mail Stop 416  
Denver Federal Center  
Lakewood, Colorado 80225

Copies of this report can be  
purchased from:

Open-File Services Section  
Western Distribution Branch  
U.S. Geological Survey  
Box 25425, Federal Center  
Lakewood, Colorado 80225  
(Telephone: [303] 234-5888)

## CONTENTS

	Page
Abstract-----	1
Introduction-----	2
Acknowledgments-----	4
Previous work-----	5
Geology of the study area-----	6
Conceptual model-----	11
Recharge and boundary flux-----	12
Ground-water basins-----	13
Oasis Valley ground-water basin-----	15
Alkali Flat-Furnace Creek Ranch ground-water basin-----	15
Ash Meadows ground-water basin-----	17
Uncertainty in the conceptual model-----	20
Modeling technique-----	21
Inverse procedure-----	21
Model mesh-----	23
Boundary conditions-----	25
Hydraulic-head measurements-----	26
Assumptions made during the study-----	28
Variables and parameters-----	29
Model results-----	31
Simulated hydraulic heads-----	31
Description-----	31
Discussion-----	34
Sources of error-----	34
Distribution of residuals-----	35
Measures of fit of simulated with measured hydraulic heads-----	35
Values of parameters-----	36
Description-----	36
Transmissivities-----	36
Carbonate rocks-----	37

CONTENTS--Continued

	Page
Tuffs-----	40
Clastic rocks and argillite-----	40
Rocks beneath the Amargosa Desert-----	41
Fluxes-----	41
Standard errors-----	42
Calculated fluxes-----	43
Sensitivity analyses-----	43
Hydraulic-head analysis-----	45
Procedure-----	45
Results and discussion-----	47
Summary-----	53
Flux analysis-----	55
Procedure to calculate flux sensitivity-----	55
Results and discussion-----	57
Summary-----	64
Conclusions-----	65
References cited-----	67

ILLUSTRATIONS

[Plate is in pocket]

Plate 1. Map showing distribution of hydraulic heads, model residuals, zones, and sites of unit-flux calculations, Nevada Test Site and vicinity, Nevada-California.

	Page
Figures 1-5. Maps showing:	
1. Generalized geology-----	3
2. Mesh and zones used in regional, two-dimensional flow model-----	24
3. Simulated hydraulic heads-----	33
4. Scaled hydraulic-head sensitivities with respect to the flux of zone 24-----	51

ILLUSTRATIONS--Continued

	Page
5. Scaled hydraulic-head sensitivities with respect to the transmissivity of zone 19-----	54

TABLES

	Page
Table 1. Summary of hydrologic units-----	8
2. Initial estimates and coefficients of variation of model parameters-----	32
3. Values of model variables and standard errors-----	38
4. Gradient, transmissivity, and unit-flux calculations for sites pertinent to a hypothetical repository located in the southwest quadrant of the Nevada Test Site-----	44
5. Summary of scaled hydraulic-head sensitivities-----	48
6. Summary of flux sensitivities scaled by value of parameter and inverse flux-----	58
7. Summary of flux sensitivities scaled by estimated standard error of parameter and inverse flux-----	62

TWO-DIMENSIONAL, STEADY-STATE MODEL OF GROUND-WATER FLOW,  
NEVADA TEST SITE AND VICINITY, NEVADA-CALIFORNIA

---

By Richard K. Waddell

---

ABSTRACT

A two-dimensional, steady-state, finite-element model of the ground-water flow system of the Nevada Test Site and vicinity in Nye and Clark Counties, Nevada, and Inyo County, California, was developed using parameter-estimation techniques. The model simulates flow in an area underlain by clastic and carbonate rocks of Precambrian and Paleozoic age, and volcanic rocks and alluvial deposits of Tertiary and Quaternary age. Normal Basin-and-Range faulting and both right- and left-lateral strike-slip faults have caused the juxtaposition of rocks of differing hydraulic conductivities.

Characteristics of the flow system are principally determined by locations of low-hydraulic-conductivity rocks (barriers); by amounts of recharge originating in the Spring Mountains, Pahrnagat, Timpahute, and Sheep Ranges, and in Pahute Mesa; and by amount of flow into the study area from Gold Flat and Kawich Valley. Discharge areas (Ash Meadows, Oasis Valley, Alkali Flat, and Furnace Creek Ranch) are upgradient from barriers. Analyses of sensitivity of hydraulic head with respect to model-parameter variations indicate that the flux terms having the greatest impact on model output are recharge on Pahute Mesa, underflow from Gold Flat and Kawich Valley, and discharge at Ash Meadows. The most important transmissivity terms are those for rocks underlying the Amargosa Desert (exclusive of Amargosa Flat area), the Eleana Formation along the west side of Yucca Flat, and the Precambrian and Cambrian clastic rocks underlying the Groom Range.

Sensitivities of fluxes derived from simulated heads and head sensitivities were used to determine the parameters that would most affect predictions of radionuclide transport from a hypothetical nuclear repository in the southwest quadrant of the Nevada Test Site. The important parameters for determining flux through western Jackass Flats and Yucca Mountain are

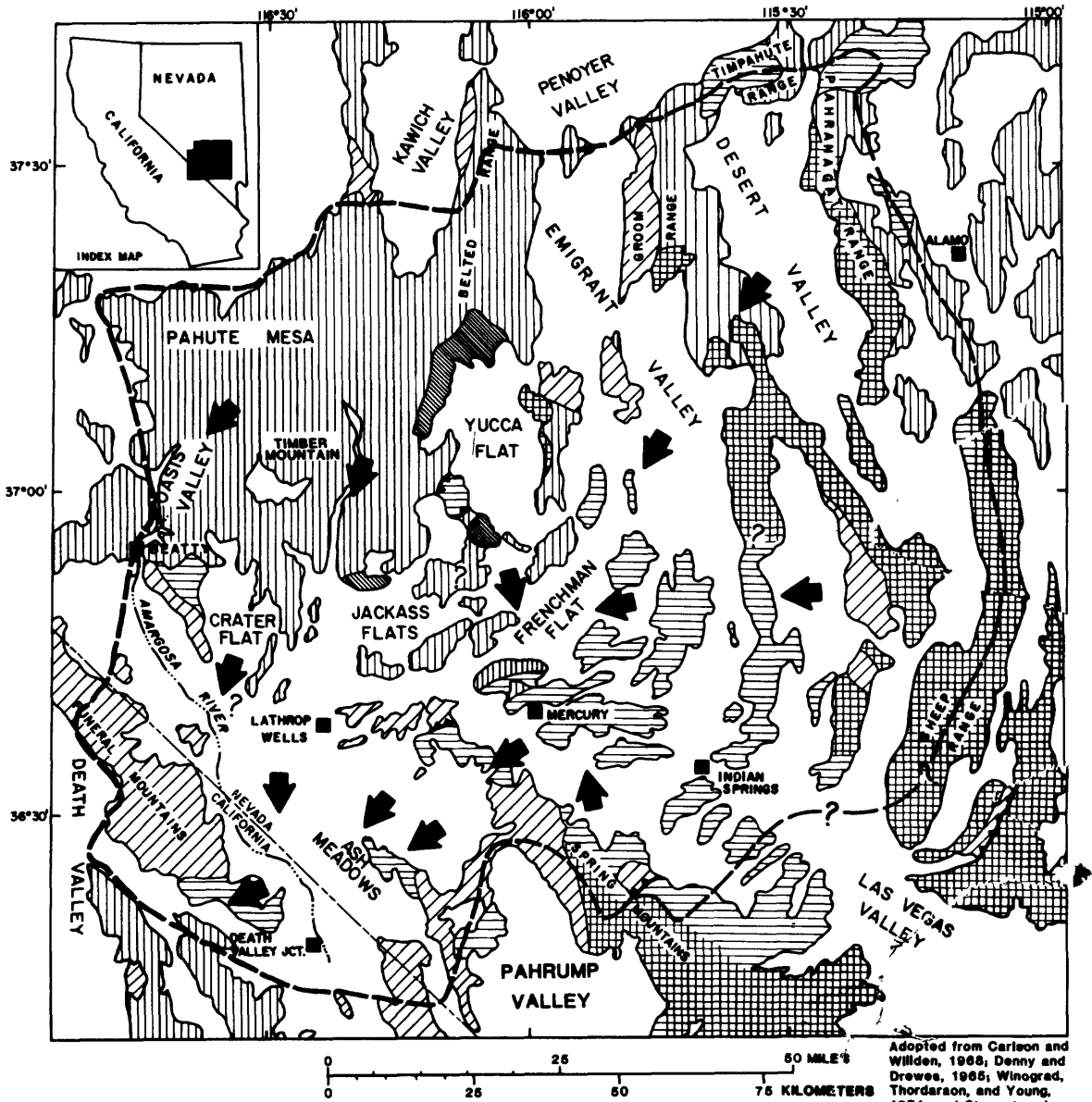
recharge to and underflow beneath Pahute Mesa; and transmissivities of the Eleana Formation, clastic rocks underlying the Groom Range, tuffs underlying Fortymile Canyon, and tuffs beneath Yucca Mountain. In the eastern part of Jackass Flats, the important parameters are transmissivities of the Eleana Formation; clastic rocks underlying the Groom Range; transmissivity of tuffs beneath Fortymile Canyon; and recharge or discharge terms for Pahute Mesa, Ash Meadows, and the Sheep Range. Transmissivities of rocks beneath the Amargosa Desert are important for flux calculations there.

## INTRODUCTION

The disposal of high-level radioactive wastes produced by commercial nuclear reactors is an aspect of the nuclear fuel cycle that currently (1982) has high national interest. The Nevada Nuclear Waste Storage Investigations, funded by the U.S. Department of Energy under Interagency Agreement DE-AI08-78ET44802, are designed to appraise the Nevada Test Site for potential repository sites. These investigations include non-site-specific experiments on various rock types, and regional and site-specific geologic, geophysical, and hydrologic investigations.

One of the more probable mechanisms for transport of radionuclides from a repository to the biosphere is transport by ground water. This report documents results of an investigation of the regional hydrology of the Nevada Test Site and vicinity, which was conducted using computer-simulation techniques. Analyses of effects near the potential repository site in the southwest quadrant of the Nevada Test Site and of transport of radionuclides are aspects of the hydrologic investigations planned for future work.

The Nevada Test Site is located in Nye County, Nevada. The study area of about 18,000 km<sup>2</sup> (square kilometers) (pl. 1, fig. 1), however, encompasses parts of Clark, Nye, and Lincoln Counties, Nevada, and Inyo County, California. The study area's boundaries are determined by areal distribution of precipitation or lithology. Altitudes range from greater than 3,600 m (meters) in the Spring Mountains (Charleston Peak) to below sea level in Death Valley. Climatic conditions vary with altitude; precipitation ranges from less than 50 mm/yr (millimeters per year) in Death Valley to greater than 700 mm/yr in the Spring Mountains.



EXPLANATION

- |   |   |   |   |
|---|---|---|---|
| QUATERNARY  |   |  | Lower carbonate aquifer                     |
|  | Alluvium, lake beds, and minor volcanic rocks                                   | PALEOZOIC (CAMBRIAN)-PRECAMBRIAN  |   |
| TERTIARY  |   |  | Lower clastic aquitard                      |
|  | Tuff, rhyolite, and associated volcanic rocks                                   | SYMBOLS   |   |
| MESOZOIC (Minor -- not shown)   |   |  | Contact                                     |
| PALEOZOIC   |   |  | Thrust fault                                |
|  | Undifferentiated upper clastic aquitard, and lower and upper carbonate aquifers |  | Approximate boundary of ground-water system |
|  | Upper clastic aquitard  |  | Approximate direction of ground-water flow  |

Figure 1.--Generalized geology.

The goals of this investigation were: (1) To estimate ground-water fluxes for use in predictions of transport of radionuclides; and (2) to study the effects of uncertainty in model parameters on these estimates. An understanding of the regional flow of ground water near a repository site is essential before risk analyses can be completed for that site. Both regional and repository-scale models need to be used to estimate the transport of radionuclides in ground water over long distances. These models require specification of realistic boundary conditions that can be provided best from regional studies.

The following methods were used in this study:

1. Comprehensive review of published and unpublished geologic and hydrologic data for the study area;
2. Design of a conceptual model of the regional flow system and development of a mathematical description of that model;
3. Solution of the equations describing ground-water flow, based on the mathematical description of the conceptual model, using finite-element techniques;
4. Refinement of the conceptual model based on the results of the computer simulations, geologic and hydrologic knowledge, and sensitivity analysis;
5. Repetition of steps 3 and 4 until satisfactory agreement of simulated and measured values was obtained; and
6. Examination of results.

Details of these methods are provided in later section of this report.

#### ACKNOWLEDGMENTS

The author would like to thank the U.S. Department of Energy, which provided financial support for this study. William Thordarson and D. I. Leap are thanked for help in compiling and checking hydrologic data; as is R. L. Cooley for providing the computer code used in the study, giving assistance in the use of the parameter estimation, and suggesting improvements to the manuscript. The author is also indebted to Messrs. W. E. Wilson, J. M. Gerhart, I. J. Winograd, and R. J. Sun for their technical and editorial suggestions.

## PREVIOUS WORK

The report of Winograd and Thordarson (1975) is a comprehensive description of the hydrology of the study area. Their work, funded by the former U.S. Atomic Energy Commission (presently the U.S. Department of Energy), was concerned primarily with developing an understanding of the flow system, so predictions subsequently could be made of the movement of radionuclides placed in ground water by tests of nuclear weapons. Much of their work involved, but was not limited to, regional study of carbonate rocks, where highest ground-water velocities might be expected; study of volcanic rocks beneath Yucca Flat, where the majority of weapons tests had been conducted; and effects of hydrologic barriers on the flow system.

Funded by the U.S. Atomic Energy Commission, Blankennagel and Weir (1973) studied the geohydrology of the eastern part of Pahute Mesa, which is underlain by thousands of meters of tuffs and other volcanic rocks. Hydrologic tests performed in Pahute Mesa provided a basis for estimating hydraulic conductivities of volcanic rocks throughout parts of the present study area, where limited hydrologic testing had been performed, or no testing at all.

Studies by various geologists (Lipman, Christiansen, and O'Connor, 1966; Byers and others, 1976; Orkild and others, 1968) of the U.S. Geological Survey were concerned primarily with volcanic history in the Nevada Test Site area. These studies provide an excellent, though not complete, description of structural and stratigraphic details of the western part of the Nevada Test Site. Volcanic history in the region is very complex, and subsurface control is sparse to non-existent in areas other than Pahute Mesa and Yucca Flat.

Many reports on hydrology of parts of the study area have been published. A selected listing of these includes: Amargosa Desert area (Walker and Eakin, 1963; Naff, 1973); Death Valley (Hunt and others, 1966, Pistrang and Kunkel, 1964; Miller, 1977); Ash Meadows flow system (Winograd and Pearson, 1976; Winograd and Thordarson, 1975; Dudley and Larson, 1976; and Naff, Maxey, and Kaufmann, 1974); and Oasis Valley (Malmberg and Eakin, 1962; White, 1979). In addition, reports by Rush (1970) and Eakin, Schoff, and Cohen (1963) summarize hydrology of the study area.

Calibration of a flow model requires measurements of hydraulic potential at numerous points throughout the system; these data need to be interpreted on the basis of hole construction, use, and lithology. These types of data have been compiled by Thordarson, Young, and Winograd (1967); Thordarson and Robinson (1971); D. I. Leap, R. K. Waddell, and William Thordarson (U.S. Geological Survey, written commun., 1979); and by the U.S. Geological Survey WATSTORE files (Hutchinson, 1975).

#### GEOLOGY OF THE STUDY AREA

Rocks within the study area range in age from Precambrian through Holocene, and include carbonate and clastic rocks deposited in rift zones and back-arc basins, magmatic rocks associated with subduction zones, volcanic rocks associated with both subduction zones and oceanic ridges, and alluvial and lacustrine deposits filling valleys created by Basin-and-Range faulting. Combinations of normal, reverse, and strike-slip faulting, and folding episodes have resulted in complex distributions of rocks. Burchfiel and Davis (1972, 1975); Christiansen and Lipman (1972); Dickinson (1977); Lipman and others (1972); Poole and Sandberg (1977); Poole, Sandberg, and Boucot (1977); Stewart and Sucek (1977); and Stewart (1980) provide models for tectonic evolution of the western United States.

Winograd and Thordarson (1975) provide an excellent framework for discussing geohydrology of the study area. Unless otherwise noted, terminology and estimates of transmissivity and thickness are from their report. Stratigraphy in the study area is summarized in table 1.

The oldest rocks of hydrologic significance within the study area are Precambrian and Lower Cambrian quartzites and shales (thickness approximately 3,000 m) that, with the lower part of the overlying Carrara Formation, compose the lower clastic aquitard of Winograd and Thordarson (1975). (An aquitard is a body of rock that has low but measureable hydraulic conductivity, and, therefore, impedes the flow of water. Where an aquitard is in stratigraphic juxtaposition to an aquifer and retards ground-water movement into or from the aquifer, it functions as a confining bed, as defined by Lohman and others (1972). The more specific term, confining bed, is preferred by the U.S.

Geological Survey, where both hydraulic and stratigraphic conditions warrant its use.) Sediments from which these rocks were formed were deposited during formation of a rift zone. Transmissivity of this hydrologic unit is approximately  $1 \times 10^{-4} \text{ m}^2/\text{s}$  (square meters per second). Because of this small value, the unit significantly affects distribution of hydraulic potential and locations of discharge areas.

The Carrara Formation is a transitional lithology consisting of siltstones near its base and limestones toward its top. The formation represents the shift toward continental shelf-and-slope conditions in the eastern part of the Cordilleran miogeocline. The upper part of the Carrara and the limestones and dolomites of Cambrian, Ordovician, Silurian, and Devonian age comprise the lower carbonate aquifer. This aquifer is widespread in the eastern part of the study area, and is the major water-transmissive unit there. Major stratigraphic units within this hydrologic unit include the Bonanza King Formation, Nopah Formation, Pogonip Group, Nevada Formation, and Devils Gate Limestone. Total thickness exceeds 4,700 m, and transmissivities range from  $1 \times 10^{-4}$  to  $0.5 \text{ m}^2/\text{s}$ . These rocks were deposited under submarine through subaerial environments. Dolomitization has changed the character of much of the rock; this may have been the result of mixing fresh and sea water in a paleo-groundwater system, as discussed by Dunham and Olson (1978). Dolomites are more prevalent in the eastern part of the area. Because they are less soluble than limestones, secondary permeability may be less well-developed in the east; however, insufficient data exist to test this hypothesis. Because of the high values of transmissivity of this hydrologic unit, hydraulic gradients are small.

The Antler orogeny caused a major shift to clastic deposition in northern Nevada. In southern Nevada, a less significant shift to clastic deposition occurred, resulting in deposition of the Chainman Shale and the Eleana Formation (Devonian and Mississippian age); the Eleana Formation apparently was deposited only in the vicinity of the Nevada Test Site. To the east, limestones of equivalent age are present in the Spring Mountains. Little is known of the transition. The Eleana consists primarily of argillite, with some quartzite and limestone, is approximately 2,400 m thick, and has a transmissivity of  $1 \times 10^{-4} \text{ m}^2/\text{s}$  or less. The low value of transmissivity

Table 1.--Summary of hydrologic units

Hydrologic unit	Geologic unit	Age	Tectonic/Sedimentary setting	Approximate transmissivity (square meters per second)
Alluvial aquifer	Numerous stream and alluvial fan gravels	Quaternary and Tertiary	Filling of basins created by basin-and-range and strike-slip faulting	$1 \times 10^{-4}$ to $5 \times 10^{-3}$
Lacustrine confining beds	Various lake bed deposits of silts and clays	Quaternary and Tertiary	Playa lakes	$< 1 \times 10^{-4}$
Tuffaceous aquifers and confining beds	Numerous units. Important aquifers include Paintbrush and Timber Mountain Tuffs, and basalts and rhyolitic flows	Tertiary	Oligocene and Miocene volcanism resulted from subduction of plate. Later activity associated with the overridding of oceanic ridge systems	$7 \times 10^{-5}$ to $1 \times 10^{-2}$
Minor confining bed	Granitic stocks	Cretaceous through Permian	Magmatic activity caused by subduction of oceanic rocks beneath North American plate	(Not regionally significant)
Upper carbonate aquifer	Tippipah Limestone	Permian and Pennsylvanian	Shelf-and-slope environment following erosion of Antler Highland	(Not regionally significant)

Table 1.--Summary of hydrologic units--Continued

Hydrologic unit	Geologic unit	Age	Tectonic/Sedimentary setting	Approximate transmissivity (square meters per second)
Upper clastic aquitard	Eleana Formation (argillite, quartzite, limestone)	Mississippian and Late Devonian	Deep-water (?) deposition of sediments off Antler Highland, within the back-arc basin	$< 1 \times 10^{-4}$
Lower carbonate aquifer	Devils Gate Limestone, Nevada Formation, Pogonip Group, Nopah Formation, Bonanza King Formation, and Carrara Formation (limestones and dolomites)	Middle Cambrian to Late (?) Devonian	Shelf-and-slope environment, east side of back-arc basin	$1 \times 10^{-4}$ to $5 \times 10^{-1}$
Lower clastic aquitard	Carrara Formation, Zabriskie Quartzite, Wood Canyon Formation, Stirling Quartzite, and Johnnie Formation (quartzites and shales)	Early Cambrian and Precambrian	Rift zone	$1 \times 10^{-4}$

makes the Eleana one of the important hydrologic units, similar to the underlying lower clastic aquitard. Winograd and Thordarson refer to the Eleana as the upper clastic aquitard.

Completion of erosion of the Antler Highland resulted in a shift back to deposition of carbonate sediments. The Tippipah Limestone of Pennsylvanian and Permian age formed from these sediments. Called the upper carbonate aquifer, it is of minor hydrologic significance, because it is saturated only in western Yucca Flat; or, where the Eleana is absent, the aquifer is not hydrologically separable from the underlying lower carbonate aquifer.

Granitic bodies of Mesozoic age occur at the northern end of Yucca Flat. They are small, and are not of great significance to regional hydrology.

Tuffs and other volcanic rocks of Tertiary and Quaternary age have varied hydrologic properties. These rocks are associated with Tertiary-age eruptive centers (Silent Canyon, Claim Canyon, Black Mountain, Sleeping Butte, Oasis Valley, and Timber Mountain) in the northwestern and western parts of the study area, and Quaternary-age basalt cones in Crater Flat. Aggregate thickness is unknown, but exceeds several thousand meters. Stratigraphy of the tuffs is complex. Rock properties are dependent not only on eruptive history, but also on cooling history, post-depositional mineralogic changes, and structural setting. Permeability of ash-flow tuffs is in part a function of the degree of fracturing, and, thus, the degree of welding (Winograd, 1971; Blankennagel and Weir, 1973). Densely welded tuffs fracture readily; airfall tuffs do not. Therefore, distribution of permeability is affected by irregular distribution of different tuff lithologies and is a function of proximity to various eruptive centers. Permeability also is a function of proximity to faults and fracture zones. An additional complication is provided by chemistry of the water in the tuff as a function of position along a flow line (Claassen and White, 1979). At the upper end of the flow line, dissolution of glass results in a sodic water with high calcium content. Farther down the flow path, zeolites and clays precipitate, and calcium content decreases. Precipitation of these minerals in the fractures decreases permeability.

Valley-fill material consists of alluvial fan, fluvial, fanglomerate, lakebed, and mudflow deposits (Winograd and Thordarson, 1975, p. 37). Alluvial

fan, fluvial, and fanglomerate deposits are composed primarily of sand, gravel, and cobbles; therefore, they have higher values of hydraulic conductivity than lakebed and mudflow deposits do, which contain clay-sized material. Fine-grained deposits may be expected to have conductivities several orders of magnitude smaller than sands and gravels. Transmissivities for alluvial-fill deposits ranging from  $1.1 \times 10^{-4} \text{ m}^2/\text{s}$  to  $4.9 \times 10^{-3} \text{ m}^2/\text{s}$  were reported by Winograd and Thordarson (1975, table 3).

Distribution of valley-fill material is a function of distance from source, relationship to alluvial channels, type of source material, and position of the water table at the time of deposition. Grain size decreases from proximal to distal ends of alluvial fans, and away from distributary channels on the fans. Because intensity of runoff varies from event to event, interbedding of fine- and coarse-grained material occurs in valley fill. This results in vertical hydraulic conductivities that are much lower in value than horizontal conductivities. Lakebeds are deposited where stream gradients are small enough that the streams only rarely are capable of carrying other than fine-grained material. Yucca and Frenchman Flats are closed basins, so lakebeds are present in the lowest parts of these basins. In the present-day Amargosa Desert, lakebeds may be forming in a small area north of Eagle Mountain. Denny and Drewes (1965) mapped extensive lakebed deposits of Pleistocene age throughout much of the Amargosa Desert. The most probable explanation for widespread occurrence of these lakebeds is an increase in elevation of the water table during pluvial periods of the Pleistocene (I. J. Winograd, U.S. Geological Survey, oral commun., 1981). Winograd and Doty (1980) have documented a higher water table northeast of Ash Meadows spring lineament during the late (?) Pleistocene.

#### CONCEPTUAL MODEL

Major elements of the conceptual model of the ground-water flow system are recharge/discharge fluxes, boundary fluxes, and distribution of hydrologic properties of geohydrologic units. The conceptual model used in this study is based largely on that proposed by Winograd and Thordarson (1975); it has been refined by use of data not available to them, especially data obtained from

recently drilled holes. The types of data used in developing the conceptual model include geologic information; water-level information (obtained from drill holes and spring altitudes); precipitation data; measurements of discharge of springs; aquifer-test data; water chemistries; and surface and subsurface geophysical information.

### Recharge and Boundary Flux

Quiring (1965) presented evidence that a linear relationship with a positive slope between the logarithm of normalized precipitation and altitude exists in the study area. Precipitation-gaging stations were classified into one of two categories, excess and deficient, based on their relationship to the precipitation-versus-altitude curve for all stations combined. Deficient stations are located in valleys, where topographic slope is gentle and rate of orographic rise is slow; precipitation occurs over fairly large areas. Excess stations are located where topography is steep; rapid orographic rise causes precipitation to be concentrated, resulting in greater amounts of precipitation than would be expected if altitude were the only factor.

An isohyetal map of the study area (Winograd and Thordarson, 1975, fig. 3, modified from Quiring, 1965) shows that mean annual precipitation ranges from 45 mm/yr (Death Valley) to greater than 700 mm/yr (Spring Mountains). The areas of greatest precipitation are the Sheep Range and Spring Mountains in the east; and Black Mountain, Pahute Mesa, the Belted Range, the Groom Range, and the Pahrnagat Range in the north.

Isohyetal maps have been used to estimate amounts of recharge in the southern Great Basin. Empirical precipitation-recharge relationships developed from mass-balance estimates for many basins in southern Nevada by Eakin, Schoff, and Cohen (1963) and Walker and Eakin (1963) suggest that no recharge occurs where mean annual precipitation is less than about 200 mm (millimeters); Rush (1970) would place the limit at about 150 mm. These empirical relationships reflect the idea that, as precipitation increases, the percentage of precipitation that is recharge also increases.

As pointed out by Winograd and Friedman (1972) and Winograd and Thordarson (1975), the use of isohyetal maps for estimating amounts of

recharge can lead to large errors. Differences in underlying lithology, thickness of soil zone, and topography are ignored in empirical relationships. In simulations, the isohyetal map was used to determine areas where recharge is most likely to occur, and to assign initial estimates of recharge for use in the parameter-estimation procedure. In the Groom Range, where the lower clastic aquitard is the predominant hydrostratigraphic unit present, recharge was estimated to be much lower than in areas of similar amounts of precipitation underlain by carbonate or tuffaceous rocks.

Winograd and Friedman (1972), estimate that as much as 35 percent of the discharge at Ash Meadows may be from Pahrangat Valley. This estimate is based on differences in deuterium contents of water from Pahrangat Valley, the Spring Mountains and Sheep Range, and Ash Meadows.

Head relationships between Pahrump Valley and the southern Amargosa Desert require ground water to flow into the study area from Pahrump Valley. The gradient is steep (approximately 0.08) across the Resting Springs Range, which is composed of low-permeability clastic rocks of Precambrian and Early Cambrian age; flux across this boundary is small.

Blankennagel and Weir (1973) estimate that approximately  $0.22 \text{ m}^3/\text{s}$  (cubic meter per second) enter the ground-water system beneath eastern Pahute Mesa from Gold Flat and Kawich Valley. This estimate is based on estimates of recharge to these valleys by Eakin, Schoff, and Cohen (1963), estimates of underflow into these valleys from the north, and estimates of proportions of discharge from these valleys that flow beneath Pahute Mesa.

#### Ground-Water Basins

The study area is composed of parts of three ground-water basins (Ash Meadows, Oasis Valley, and Alkali Flat-Furnace Creek Ranch) (pl. 1). These basins are defined as those areas that contribute water to discharge at their respective discharge areas; they include recharge and discharge areas, and areas under which water must flow from one to the other. Because boundaries of these three basins are not well-known, parts of each have been included in the model; the relationship of the model to these basins is discussed below.

Winograd and Thordarson (1975) subdivided the ground-water system into the Ash Meadows ground-water basin and the Oasis Valley-Fortymile Canyon

ground-water basin. The Ash Meadows ground-water basin is composed of those areas that contribute ground water to the springs at Ash Meadows. Similarly, the Oasis Valley-Fortymile Canyon basin is composed of those areas that contribute to discharge at Oasis Valley and ground-water flow beneath the area between Oasis Valley and Fortymile Canyon. Because ground water flowing beneath Fortymile Canyon does not discharge there, but does discharge at Alkali Flat, and perhaps in Death Valley near Furnace Creek Ranch, it is more convenient to define an Alkali Flat-Furnace Creek Ranch ground-water basin. The Oasis Valley ground-water basin consists of those areas that contribute water to discharge in Oasis Valley. Note that this basin does not include all the area included in Winograd and Thordarson's (1975) Oasis Valley-Fortymile Canyon ground-water basin; the Fortymile Canyon part of their basin is part of the Alkali Flat-Furnace Creek Ranch basin defined here.

Ash Meadows and Oasis Valley ground-water basins are in fact subbasins within the Alkali Flat-Furnace Creek Ranch basin. These two discharge areas are caused by rocks of low hydraulic conductivity, forcing water levels high enough to intersect the ground surface, forming springs. Because these ground-water dams have low, but non-zero, hydraulic conductivities, water flows through these dams. At Oasis Valley, water also can flow through alluvium over the "spillway" created by the lower clastic aquitard, and never leave the ground-water system. The possibility of water flowing through alluvium also exists at Ash Meadows; many of the springs emerge from alluvium. In both areas, water discharged from springs, if not used for irrigation, only flows a short distance on land surface, until it is either removed completely from the ground-water system by evapotranspiration, or it reenters the ground-water system by moving downward into the alluvium. This amount of water that reenters the ground water is probably small, because of high demand for water by plants in desert environment. Because of uncertainties in hydraulic conductivities and thickness of ground-water dams in the amount of evapotranspiration, and in the amount of flow over and through the spillways, contributions of the Oasis Valley and Ash Meadows ground-water basins to the Alkali Flat-Furnace Creek Ranch basin are unknown. Because discharge areas are caused by low-conductivity rocks, and because of arid environment, these contributions are probably small.

In a manner analogous to the Oasis Valley and Ash Meadows ground-water basins being tributaries to the Alkali Flat-Furnace Creek Ranch basin, Alkali Flat-Furnace Creek Ranch basin is a tributary to Death Valley basin. Not only is Furnace Creek Ranch within Death Valley, but the Alkali Flat discharge area is caused by the presence of low-conductivity rocks downgradient from the discharge area. Rocks of the lower clastic aquitard crop out at Eagle Mountain. Both leakage of water through this dam, and movement over the spillway through alluvium in the Amargosa River, probably occur.

#### Oasis Valley Ground-Water Basin

Discharge at Oasis Valley is caused by the presence of low-conductivity rocks downgradient from Beatty, as noted above. The discharge has been estimated to be  $0.078 \text{ m}^3/\text{s}$  (Malmberg and Eakin, 1962). Water flows into Oasis Valley from western and central Pahute Mesa. The boundary between the Oasis Valley basin and the northern part of the Alkali Flat-Furnace Creek Ranch basin is not well-known, but extends approximately from Beatty to the northeast along Beatty Wash and into eastern Pahute Mesa. The subbasin is small, extending only about 70 km (kilometers) north-south and about 20 km east-west.

The Oasis Valley basin contains volcanic rocks, unconsolidated alluvial and perhaps lacustrine deposits, Proterozoic and Paleozoic clastic and carbonate rocks, and granitic rocks at depth. Volcanic rocks dominate the subbasin. Paleozoic and Proterozoic rocks crop out only locally in the Bullfrog Hills just west of Oasis Valley, and at the southwest edge of the basin at Beatty, and probably do not greatly affect the flow of ground water. Alluvium is locally important as an aquifer in Gold Flat. Granitic rock was encountered in a drill hole in central Pahute Mesa (J. W. Hasler and F. M. Byers, Jr., U.S. Geological Survey, written commun., 1965), and may underlie Black Mountain.

#### Alkali Flat-Furnace Creek Ranch Ground-Water Basin

The northern boundary of this basin, which includes Yucca Mountain, is along a line that crosses the Cactus, Kawich, and Reveille Ranges. The eastern boundary is well established in the northern part, where it lies along

a line running through the axes of the Reveille and Belted Ranges. Southward, the boundary is more obscure. Water flows eastward across a barrier (composed of the upper clastic aquitard along the west side of northern Yucca Flat), but it is not known whether this water discharges at Ash Meadows or flows beneath Rock Valley and eastern Jackass Flats. The boundary with the Ash Meadows basin is well-known near Ash Meadows, extending from the Skeleton Hills northeastward to the northern end of the Specter Range. From there, its location is uncertain. Because of the low hydraulic conductivity of the upper clastic aquitard, little water flows across it, so that the boundary question is of minor importance.

The geologic cross section (pl. 1) extending from Pahute Mesa to Alkali Flat and Eagle Mountain shows that the northern part of the basin is underlain by volcanic rocks associated with several caldera systems. Both Basin-and-Range style faults and faults associated with caldera formation are present.

Granitic rocks probably underlie most of the caldera areas (Byers and others, 1976, fig. 3), but the potential gradient across Timber Mountain caldera is low (fig. 5.6-1). The low gradient may be caused by high-permeability volcanic rocks, in which case granitic rocks must be too deep to affect the "shallow" ground-water system, and (or) by an appropriate amount of recharge occurring near Timber Mountain, or by both.

The southern part of the basin is underlain mostly by unconsolidated deposits. Approximately 10 km north of Lathrop Wells, part of the alluvium is saturated with water, and from there downgradient to Alkali Flat the alluvium transmits most of the ground water. Aeromagnetic data (Greenhaus and Zablocki, 1982) show that volcanic rocks are scarce beneath the Amargosa Desert. Presumably Paleozoic or Precambrian rocks underlie the alluvium, but many details of their lithology and structure are unknown. In a 467-m deep hole (AM-101) in alluvium near Lathrop Wells, depth to water is approximately 73 m; the saturated alluvium is thus at least 394 m thick. Downgradient, the depth to water progressively decreases until it is only a few meters at Death Valley Junction. Certainly flow in the alluvium is important, but the role of the Paleozoic and Precambrian rocks beneath the alluvium is unknown.

Paleozoic carbonate rocks are present in the southern part of the Funeral Mountains northwest of Death Valley Junction. Springs near Furnace Creek

Ranch at the east edge of Death Valley discharge water from these carbonate rocks, either directly from the carbonate rocks or from alluvium overlying them. Some of the springs are several hundred meters above the floor of Death Valley. Lakebeds or impermeable zones developed along the Furnace Creek fault system may form barriers causing the water to discharge some distance up the slope rather than at the base.

Origin of water discharged in the Furnace Creek Ranch area is uncertain, but its chemistry strongly resembles that of water in the alluvium in the central Amargosa Desert (Winograd and Thordarson, 1975, p. C112). Water discharging at Furnace Creek Ranch is probably a mixture of water from all three basins.

Discharge by evapotranspiration at Alkali Flat has been estimated (Walker and Eakin, 1963) to be  $0.39 \text{ m}^3/\text{s}$ ; flow across the barrier at Eagle Mountain is estimated to be about  $0.02 \text{ m}^3/\text{s}$ . Discharge near Furnace Creek Ranch was estimated to be about  $0.20 \text{ m}^3/\text{s}$  (Hunt and Mabey, 1966). Total flux in the Alkali Flat-Furnace Creek Ranch basin (not counting the discharge in the Oasis Valley and Ash Meadows basins) is estimated to be about  $0.61 \text{ m}^3/\text{s}$ , or  $53,000 \text{ m}^3/\text{d}$  (cubic meters per day).

#### Ash Meadows Ground-Water Basin

Ash Meadows ground-water basin is in the eastern half of the study area. Flow is primarily in Paleozoic limestone and dolomite units, and is from the recharge areas in the Spring Mountains, Pahranaagat, Timpahute, and Sheep Ranges, and Pahranaagat Valley toward the Ash Meadows spring lineament. Potentiometric gradients throughout much of the basin are low, because of high transmissivities exhibited by soluble carbonate rocks. Locations of low-permeability rocks greatly affect distributions of head and directions of flow. One example of several presented by Winograd and Thordarson (1968, 1975) is the steep gradient across Las Vegas shear zone (zone 21). Springs (Indian Spring and Cactus Spring) occur along the shear zone. Right-lateral movement along the shear zone has resulted in either inclusion of low-permeability rocks within the shear zone or development of a low-permeability fault gouge. Aquifer-test data indicate that the second hypothesis is more plausible (Winograd and Thordarson, 1968, 1975).

Potentiometric data from wells in Yucca and Frenchman Flats indicates that ground water flows downward through alluvium and volcanic rocks into underlying Paleozoic carbonate rocks. This indicates that (1) the potentiometric level is lower in the carbonate rocks; (2) the carbonate rocks influence the potentiometric level in the overlying rocks; and (3) because the carbonate rocks transmit most of the water, their permeabilities must be higher than those of the overlying rocks.

Carbonate rocks transmit most of the water in the basin, but other lithologies are locally important. Northeast of the Ash Meadows spring line, the saturated thickness of alluvium may be more than 100 m. Beneath Yucca and Frenchman Flats, both alluvium and volcanic rocks are saturated. The springs at Indian Springs discharge from alluvium, though carbonate bedrock occurs nearby.

A second example of the effect of low-permeability rocks given by Winograd and Thordarson (1968, 1975) is the steep gradient across the Groom Range (zone 3), where the lower clastic aquitard is present. Here, water flowing from west (western Emigrant Valley) to east (eastern Emigrant Valley) is impeded by silica-cemented, Precambrian and Cambrian sandstones. Juxtaposition of high- and low-permeability rocks resulted from Basin-and-Range style normal faulting. The same low-permeability units also retard flow from western Emigrant Valley into Yucca Flat.

The lower end of this basin is its discharge area in Ash Meadows (zone 13); discharge is estimated to be  $0.655 \text{ m}^3/\text{s}$  (Walker and Eakin, 1963). Here again, low-permeability rocks affect the flow system. A normal fault, with movement down to the west, was discovered by a gravity survey (Healy and Miller, 1971). The fault juxtaposes low-permeability lakebed deposits (zone 23) on the downthrown side, against rocks of the lower carbonate aquifer, forcing flow lines upward (Dudley and Larson, 1974). Discharge is from springs in alluvial sediments downgradient (southwest) from the fault. Ends of the spring line are determined by occurrences of the lower clastic aquitard 10 to 15 km south-southwest of Skeleton Hills, and at the northern end of the Resting Spring Range. These low-permeability rocks form boundaries for the Ash Meadows basin between Ash Meadows and the Specter Range, so that almost all discharge at Ash Meadows must pass through a restriction beneath the

Specter Range that is only about 8-km wide. Winograd and Thordarson (1975) calculated regional transmissivities of about  $0.6 \text{ m}^2/\text{s}$  for the lower carbonate aquifer in this area, six to nine times greater than determined from aquifer tests.

Water from Pahute Mesa also flows to the south toward Crater and Jackass Flats. The Timber Mountain caldera complex is between Pahute Mesa and these areas; its effect on hydrology is unknown. The resurgent dome, Timber Mountain, is intensely fractured and faulted, but these fractures may be partially healed by precipitation of montmorillonite and (or) zeolites. Granitic dikes have been mapped on the south flank of Timber Mountain (Byers and others, 1976), and granite may be present at depth. A caldera moat surrounds the resurgent dome. This moat contains great thickness of ash-flow tuffs as well as slump deposits from walls of the caldera. Centripitally oriented ring fractures and faults are in the moat; hydrologic characteristics of these fractures are unknown.

The Claim Canyon Cauldron segment is immediately south of the Timber Mountain complex; its hydrologic properties are unknown. Comparison of head values in Pahute Mesa, Oasis Valley, and Jackass Flats suggests that a hydrologic barrier probably exists between the southern edge of Pahute Mesa and the northern edge of Jackass Flats. Whether the Claim Canyon Cauldron segment is acting as a barrier, or whether another geologic feature (such as a possible gouge zone associated with Yucca Wash or undetected occurrences of the Eleana west of Calico Hills) acts as a barrier, is not known.

Detailed geophysical studies (D. L., Hoover, U.S. Geological Survey, written commun., 1982) in western Jackass Flats provide evidence that Fortymile Canyon is a structural feature (graben ?) that extends southward through Jackass Flats into the Amargosa Desert near Lathrop Wells. Measurements of water levels in wells in Jackass Flats, Yucca Mountain, Calico Hills, and the Amargosa Desert suggest that isopotentials vee upgradient into Fortymile Canyon. The very permeable Topopah Spring Member of the Paintbrush Tuff is present in the saturated zone beneath Fortymile Wash in western Jackass Flats, creating a zone of high transmissivity. This transmissivity may have been further increased by fractures parallel to the north-trending normal faults that created the graben. Wells J-12 and J-13 in this zone have high transmissivities (Winograd and Thordarson, 1975, table 3).

Geohydrology of Rock Valley is not well-known. Paleozoic rocks crop out on the southern edge of the valley; tuffs crop out on its northern edge. Data from Test Well F indicate that carbonate rocks are important hydrologic units near Skull Mountain. In the model, the lower carbonate aquifer was assumed to be the principal geohydrologic unit beneath Rock Valley.

Geochemical data collected by H. C. Claassen and A. F. White (U.S. Geological Survey, written commun., 1979) indicate that ground water flows to the southwest beneath Rock Valley. Water in the alluvium at Lathrop Wells is near saturation with respect to calcite and dolomite, indicating flow through carbonate rocks; water near Fortymile Wash is not close to saturation with respect to these minerals. In addition, samples near Lathrop Wells contain appreciable amounts of sulfate ion, presumably derived from alteration products near the Wahmonie intrusive on the east side of Jackass Flats. The interpretation that water beneath Rock Valley flows to the southwest, rather than to the southeast, differs from that presented by Winograd and Thordarson. The revised interpretation of the direction of flow beneath Rock Valley presented here is supported by geochemical data; potentiometric data are not sufficient to indicate which hypothesis is correct.

#### Uncertainty in the Conceptual Model

The conceptual model presented here contains many uncertainties and, therefore, so does the mathematical model. Although a great number of geologic and hydrologic studies have been done in the study area, knowledge of the study area is incomplete because of its hydrologic and geologic complexity.

Transmissivities range over several orders of magnitude, from very transmissive carbonate aquifers to poorly transmissive clastic aquitards. Distribution of transmissivity is complex. Geologic mapping shows that the Tertiary rocks have been subjected to normal, Basin-and-Range style faulting, and to both right- and left-lateral strike-slip faulting. Extensive drilling beneath Yucca Flat shows that structure beneath basins is as complex as that readily mappable in the surrounding ranges. Older Paleozoic and Precambrian rocks have undergone folding-and-thrust faulting, and perhaps gravity sliding as well. Volcanic activity and basin filling have covered much of the Paleozoic and Precambrian rock, so the structure only can be surmised from

other evidence. The presence of at least five eruptive centers has created a very complex volcanic stratigraphy. Hydraulic properties of the volcanic rocks are highly varied.

In addition to the uncertainty due to the highly complex geology, additional uncertainty also is present in locations of recharge areas and rates of recharge. Locations of boundaries of ground-water basins have been estimated from available potentiometric data, estimates of precipitation distribution, and distribution of low transmissivity rocks; therefore, these locations may be in error.

Discharge areas are generally well-known, but rates of discharge may be poorly known. It is difficult to obtain accurate estimates of discharge where numerous small springs and seeps occur, as they do near Furnace Creek Ranch and Oasis Valley. In Alkali Flat, discharge is by evapotranspiration; estimates of this discharge potentially contain larger errors. Simulated hydraulic heads, and determinations of transmissivities and recharge rates, will be affected by errors in discharge rates.

In summary, the mathematical model presented in the remainder of this report is an approximation of a conceptual model, which itself is an approximation of the ground-water system. Although the mathematical model is useful in developing an improved understanding of the system, users of the model should be aware of its deficiencies and should be cautious in their conclusions.

## MODELING TECHNIQUE

### Inverse Procedure

The numerical techniques used in this study were developed by Cooley (1977, 1979). The basic equation describing flow of ground water in porous media is given by:

$$\frac{\partial}{\partial x_i} (T_{ij} \frac{\partial h}{\partial x_j}) + R (H-h) + W = 0 \quad i, j = 1, 2 \quad (1)$$

where

$T_{ij}$  = transmissivity ( $L^2/T$ );

$R$  = hydraulic conductivity of a confining bed ( $1/T$ );

$W$  = source-sink term (positive for source) ( $L/T$ );

$h$  = hydraulic head (L);

$H$  = hydraulic head on the distal side of the aquitard (L); and

$x$  = Cartesian coordinate (L).

The repeated subscript  $i$  or  $j$  without parentheses indicates summation on that subscript. The source-sink term is composed of two different parts: The first is areally distributed recharge or discharge, depending on sign; the second is source or sink described by pumping or injection wells. This equation was solved using a finite-element code written by R. L. Cooley (U.S. Geological Survey, written commun., 1979).

Internal boundary conditions between elements are: Both specific discharge normal to the boundary and hydraulic head remain unchanged as the boundary is crossed. External boundaries may be either known flux or known head boundaries.

The code used in this study is a parameter-estimation technique described by Cooley (1977, 1979) that derives values for the parameters  $a_k$ ,  $k = 1, 2, \dots, K$ , where the  $a_k$  represent any of  $T_{ij}$ ,  $R$ , and  $W$  for zones defined throughout the modeled area. The  $a_k$  are determined to minimize the weighted sum of squared residuals of simulated head

$$\sum_{\ell=1}^I w_{\ell} e_{\ell}^2 = \sum_{\ell=1}^I w_{\ell} (h_{\ell}^{\text{obs}} - h_{\ell})^2 \quad (2)$$

where

$h_{\ell}$  = simulated head (L);

$h_{\ell}^{\text{obs}}$  = observed head (L);

$w_{\ell}$  = weighting factor;

$I$  = the number of nodes; and

$e_{\ell}$  = residual.

The weighting factor is zero, if no observation is available. The value  $h^{\text{obs}} - h$  is the residual for the node. Sums of the squared residuals are minimized by regression techniques, using a linearized regression model. An iteration scheme is used to minimize the weighted sum of squared residuals by successive approximation to model parameters. Development of a sensitivity matrix is implicit in the algorithm. Because all fluxes and transmissivities

cannot be determined from a given head distribution, some parameters used in the model must be specified as known.

A major goal in the calibration of the model was to minimize the error variance:

$$s^2 = \frac{\sum_{\ell=1}^J w_{\ell} (h_{\ell}^{\text{obs}} - h_{\ell})^2}{J-K+L} \quad (3)$$

where

J = number of observations;

K = number of parameters being estimated; and

L = number of parameters for which estimates of value exist.

Another major goal was to adjust aquifer zonation and values of parameters, so residuals were distributed randomly throughout the model area.

Success of a modeling effort is dependent on knowledge of the system, including both geometry of hydrologic units within the system and values of parameters. The better the parameters are known, the more successful the modeling effort will be. Within a system, parameters may exist where minor changes in values of these parameters do not cause significant changes in simulation results. Inverse techniques are not successful in estimating values of these parameters. On the other hand, some parameters are very important to simulation of heads; for these parameters, the inverse technique works well. The standard error of the estimated parameters reflects the ability of model to determine parameters; this error is directly dependent on the sensitivity of the model to these parameters.

#### Model Mesh

Several guidelines were used to develop the finite-element mesh and the zonation (fig. 2). The zonation must describe complex geometries found within the model area, which include barriers, aquifers, and recharge and discharge areas. Because the inverse technique uses measurements of head, nodes need to be in the same x-y position where measurements are available.

The model primarily was developed to aid in prediction of radionuclide transport from a hypothetical repository in the southwestern quadrant of the Nevada Test Site. Therefore, greater density of nodes was used in and down-

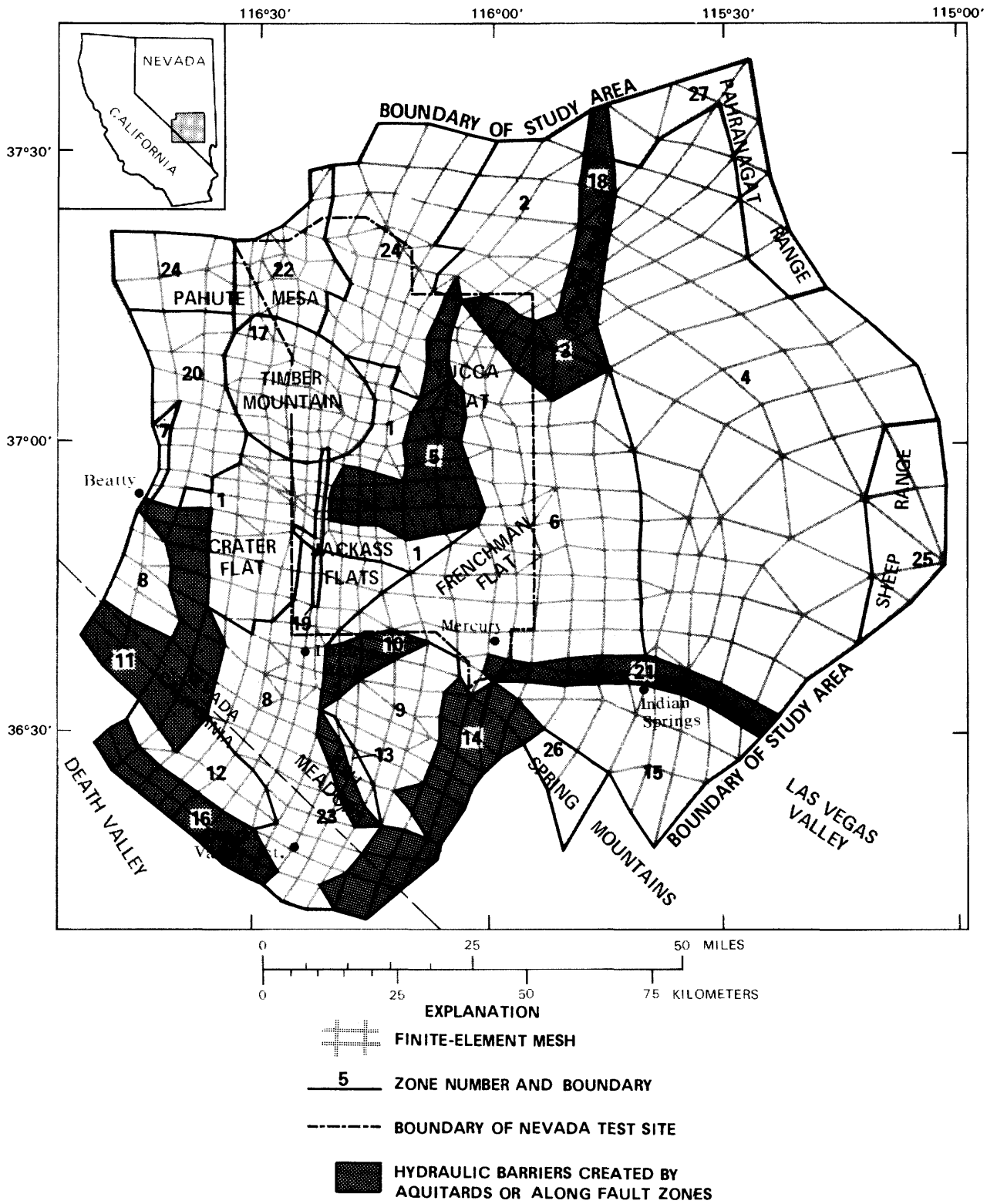


Figure 2.--Mesh and zones used in regional, two-dimensional flow model.

gradient from, the southwestern quadrant of the test site. Little is known about the hydrology or subsurface geology of part of the study area east of the Nevada Test Site and north of Las Vegas Valley (zones 4, 25, and 27); therefore, in this area, node density is sparse. During development of the mesh, it was assumed that lack of detail in this part of the model area would not have great effect on estimating heads and fluxes in the southwestern part of the study area. Sensitivity studies subsequently showed this assumption was true.

Distribution of transmissivities is important to the resulting distribution of hydraulic potential throughout the modeled area. In particular, the barriers (zones 3, 5, 10, 11, 14, 16, 18, 21, and 23) greatly affect the flow field. Zone 5 represents the Eleana Formation along the west side of Yucca Flat. The Las Vegas Valley shear zone is represented by zone 21. Zone 23 represents the barrier southwest of Ash Meadows, and zone 16 represents rocks of low transmissivity along the Furnace Creek fault zone. The other zones represent occurrences of the lower clastic aquitard.

The lower carbonate aquifer is represented by zones 4, 6, 9, 12, 13, 15, 25, 26, and 27. Tuffaceous rocks are represented by zones 1, 2, 7, 17, 20, 22, and 24. Zone 8 represents alluvium and similar deposits, but may contain tuffaceous and carbonate rocks.

Within the southwestern part of the Nevada Test Site, Fortymile Canyon (zone 19) may have a large effect on the flow of ground water within Jackass Flats. In addition, Timber Mountain (zone 17) is an area of complex geology with potentially high variability in hydrologic properties.

#### Boundary Conditions

Boundary conditions used in the model include no-flux, known-flux, and constant head boundaries. Flux boundaries are applied internally and externally to the modeled area, while the constant head boundary is applied to only one node that represents a point in Alkali Flat.

External flux boundaries correspond to areas where flux from outside the modeled area is known to occur. An area along the boundary between zones 25 and 27 represents a region where flow, Q<sub>pv</sub>, into zone 4 from Pahrnagat Valley

occurs. Another area where flux into the area is treated as a boundary flux is across part of the Resting Springs Range, where flow from Pahrump Valley into the Amargosa Desert occurs. A boundary flux out of the area was applied near Furnace Creek Ranch in Death Valley. All other external boundaries are treated as no-flow boundaries.

Internal flux boundaries represent areas of recharge or discharge. Recharge areas are represented by zones 18, 24, 25, 26, and 27. Discharge areas are represented by zones 7 and 13, and by specified nodes in zones 8 and 12. Recharge and discharge are assumed to zero elsewhere.

### Hydraulic-Head Measurements

Distribution of the 100 data points used in the simulations is shown on plate 1. A notable absence of data occurs in the northeastern part of the study area. Drill holes do not reach the saturated zone; therefore, they are usable only as a guide to indicate when simulated heads are too high. Sub-surface geology and hydrology data are insufficient in the Timber Mountain caldera complex north of Jackass Flats and south of Pahute Mesa.

A great deal of data are available in other areas. During hydrologic investigations for the weapons-testing program, two series of test holes were drilled in and around the Nevada Test Site. In addition, exploration and emplacement holes for nuclear testing have yielded large amounts of data in two areas, Yucca Flat and Pahute Mesa. Recent drilling, part of waste-disposal investigations, has given additional data in the southwestern part of the test site. Data are available in the Amargosa farm area southwest of Lathrop Wells and northeast of the Funeral Range. Numerous irrigation wells were drilled in this area; these wells are not pumped extensively at this time. Altitudes of springs in Death Valley, Ash Meadows, Oasis Valley, and Indian Springs, and of seeps in Alkali Flat and Carson Slough in the Amargosa Desert provide additional data points.

Errors in potentiometric data can have two principal sources: inaccuracy in measurements of depth to water and inaccuracy in determination of altitude of land surface. Variation in measurements of depth to water may be caused by insufficient calibration of equipment, operator error, or change in operators

and by changes resulting from seasonal evapotranspiration or pumping rates, barometric effects, and transient responses to drilling. Potentiometric data used in this study were carefully examined for quality. Depth-to-water measurements made by U.S. Geological Survey personnel working at Nevada Test Site are made with frequently calibrated equipment and with established procedures. Error in repeated measurements by different operators using different equipment is less than 0.05 percent, when measuring depths of water of about 600 m (Garber and Koopman, 1968). Altitudes of wells drilled as part of the various Nevada Test Site programs are determined by surveying; therefore, measurements of hydraulic head in these wells are considered to be quite accurate, with maximum errors of less than 1 m. Viewed in the context of the overall range in hydraulic head in the study area (greater than 1,450 m), this error is insignificant.

Errors in measurements of hydraulic head in areas other than the test site are hard to estimate. Fortunately, most of these measurements have been made in areas where numerous measurements were made in many wells (Amargosa farm area, Las Vegas Valley and Indian Springs area), and where the depth to water generally is less than 100 m. The largest component of error probably is inaccuracy in determining altitudes of measuring points. Estimated errors in measurements of hydraulic head are  $\pm 3$  m for wells in the Amargosa farm area,  $\pm 6$  m for springs in Ash Meadows and Oasis Valley, and  $\pm 12$  m for springs in Death Valley. Considering the range in heads present in the study area, significant differences in observed versus calculated heads probably are not caused by errors in measurement.

Because gradients are steep within barriers, potential for large residuals is great, and details of geometry become very important. The algorithm may generate untenable solutions because it is unable to alter the zonation, the cause of the errors. To avoid this problem, observations of head within barriers were not used, because geometrics of the barriers are not well-known. One exception is the observation in well UE25a-3, located in the Calico Hills; it was included because of the importance of data in the southwest quadrant of the Nevada Test Site. Its inclusion did not result in unrealistic solutions. Attempts to decrease the residual for this observation by modifying geometry

of the zone were generally unsuccessful, because of lack of data between Calico Hills and Timber Mountain, and the possible effect of structural features underlying Topopah Wash.

#### Assumptions Made During the Study

Several simplifications and assumptions regarding geology and hydrology were made to allow the model to be developed; many of these simplifications were necessary because of lack of data. These assumptions and simplifications were:

1. Ground-water flow is strictly horizontal. Evidence for both upward and downward flow exists beneath Pahute Mesa (Blankennagel and Weir, 1973). Beneath Yucca Flat, heads within the tuffaceous rocks are greater than in underlying carbonate rocks (Winograd and Thordarson, 1975). Although no data are available on vertical head distributions in most areas, geometric considerations indicate that flow beneath recharge areas is downward, and flow beneath discharge areas is upward. Therefore, assumption of horizontal flow eliminates the possibility of simulating the flow in these areas accurately. However, the assumption appears warranted, because: (1) Areas of greatest interest (Jackass Flats and northern Amargosa Desert) are not recharge or discharge areas, so vertical flow is not likely to be significant; (2) areas where vertical flow is significant make up a small fraction of the flow system; and (3) insufficient data exist to make a successful three-dimensional model.

2. Hydrological parameters (transmissivities, rates of recharge and discharge) do not change with time, and hydraulic heads are now at steady-state conditions. The steady-state assumption is known to be violated by the natural system. Several processes are occurring that change system characteristics with time. For example, models for evolution of ground-water chemistry imply that dissolution of rock is occurring, increasing its hydraulic conductivity, especially where carbonate rocks occur. Similarly, there is evidence that precipitation of clays and zeolite occurs in the downgradient parts of tuffaceous systems (H. C. Claassen, U.S. Geological Survey, oral commun., 1981), resulting in decreased hydraulic conductivity. These changes in conductivity occur slowly enough that hydraulic heads observed today represent

steady-state conditions. Increased recharge during past pluvial periods has resulted in slightly higher heads throughout most of the area (Winograd and Doty, 1980). Effects of pumpage are more short-lived, but are certainly important in scenarios for risk assessment.

Available data do not allow development of a transient model. In areas where pumpage has been intense (near Ash Meadows and in the agricultural area southwest of Lathrop Wells), short-term changes in water levels are documented. These changes are small in comparison to the range in heads throughout the study area. Transient data are unavailable elsewhere.

3. The rocks are isotropic with respect to hydraulic conductivity. However, very few rocks are isotropic. The mode of deposition of both sediments and tuffaceous rocks creates a definite anisotropy with respect to hydraulic conductivity, especially when vertical and horizontal conductivities are compared. Tilting of bedding converts vertical anisotropy into a strong anisotropy in horizontal directions. However, insufficient data are available from aquifer tests to evaluate the degree of anisotropy.

The effects of this simplification are: (1) Transmissivity calculated or used in the model is representative of transmissivity in the direction of flow; and (2) errors result from calculation of fluxes and directions of flow based on the concept of flow occurring perpendicular to potentiometric contours.

4. Homogeneity exists within zones. Natural materials are nonhomogeneous. The effects of assuming that zones are homogeneous are: (1) Simulated heads will not agree with measured values; and (2) predicted heads will contain uncertainties. Making zones as small as the data warrant minimizes the effects.

#### Variables and Parameters

Model variables are defined here to be material properties or boundary conditions that are required by the computer code for its use in simulating the flow system. Variables include transmissivities, distributed and point fluxes, and constant hydraulic-head values. Model parameters are defined to be model variables that have been selected for estimation by the inverse procedure. Values of parameters are changed by the inverse algorithm; all other variables are not varied.

Use of estimates of standard deviations of model parameters constrains the inverse algorithm and decreases many of the problems that exist, such as those caused by the existence of high correlations among parameters. Of the 31 variables used in the simulations, 24 were parameters that were constrained by estimating uncertainty in these parameters, and 7 were held constant.

The most important variable held constant was the estimate of discharge in the Ash Meadows discharge area. Without holding one recharge/discharge or transmissivity term constant, it is not possible to obtain estimates of other variables. The logical variable to hold constant is the one that is best-known and considered important.

Recharge values for zones 18 and 27 are treated as one parameter, even though they have different values; ratio between their values thereby will be a constant. This was done to reduce the number of parameters, while trying to maintain flexibility. These two zones represent areas with similar amounts of precipitation, but different lithologies. Zone 27 is underlain by carbonate rocks; recharge is estimated to be about 4 to 5 times that of zone 18, which is underlain by the lower clastic aquitard.

Variables for which few data are available to allow them to be estimated also were held constant. Examples are transmissivities of some of the zones representing the upper clastic aquitard (zones 10, 11, and 14). These zones primarily divert flow around them, rather than greatly retard flow. Preliminary tests showed that simulated hydraulic heads are not affected greatly by small changes in transmissivities of these zones; therefore, the inverse procedure would not be able to estimate accurately their transmissivities. Transmissivity of zone 23 is another example of a variable that cannot be estimated by the inverse procedure. This zone (23) represents lakebeds of low transmissivity that cause discharge to occur at Ash Meadows. Flux across the zone is probably small (indicated by the high gradient observed across the zone relative to gradients both upgradient and downgradient from the zone), but unknown; therefore, it is not possible to estimate a transmissivity for zone 23, using the inverse procedure. The amount of flow across the Resting Springs and Pahrangat Ranges is another example. Transmissivities of rocks beneath these ranges and the gradients across them are poorly known; therefore, these fluxes were held constant.

Values for variables were derived from available literature and unpublished data contained in files of the U.S. Geological Survey office in Lakewood, Colorado. Coefficients of variation (standard error divided by the mean) were estimated for model parameters. These reflect the amount of data available and the degree of confidence in these data for each parameter (table 2). Estimates of coefficients of variation range from 0.2 to 1.0; the larger number indicates that the parameter is not well-known and will not be tightly constrained during optimization.

Abbreviations for parameters are used in the text and tables. Transmissivity parameters are indicated by "T" followed by numbers or letters indicating the appropriate zone. Flux parameters are indicated by "Q" followed by zone number or an abbreviation. These abbreviations (and indicated areas) are "af" (Alkali Flat), "dv" (Death Valley), "rs" (Resting Springs Range), and "pv" (Pahrangat Valley).

## MODEL RESULTS

### Simulated Hydraulic Heads

#### Description

Hydraulic heads, simulated by the model, range from 1.4 m in Death Valley to 1,452 m on Pahute Mesa (fig. 3), referenced to National Geodetic Vertical Datum of 1929. High gradients (as high as  $4 \times 10^{-2}$ ) exist across the clastic rocks occurring immediately upgradient from Yucca Flat and Death Valley, and beneath the Groom Range. Intermediate and high gradients (approximately  $5 \times 10^{-3}$  to  $3 \times 10^{-2}$ ) were calculated where tuffaceous rocks occur, in the northwestern part of the study area. Low gradients (as low as  $1.6 \times 10^{-4}$ ) were calculated where carbonate rocks occur. Although the area south (upgradient) of Indian Springs is underlain by carbonate rocks, an intermediate gradient exists across this area, because significant head loss occurs across the Las Vegas Valley shear zone.

Major inflections in potentiometric contours occur between areas of greatly differing hydraulic gradients. Areas between Timber Mountain and Yucca Flat, and between Yucca Flat and the Groom Range, are notable. These

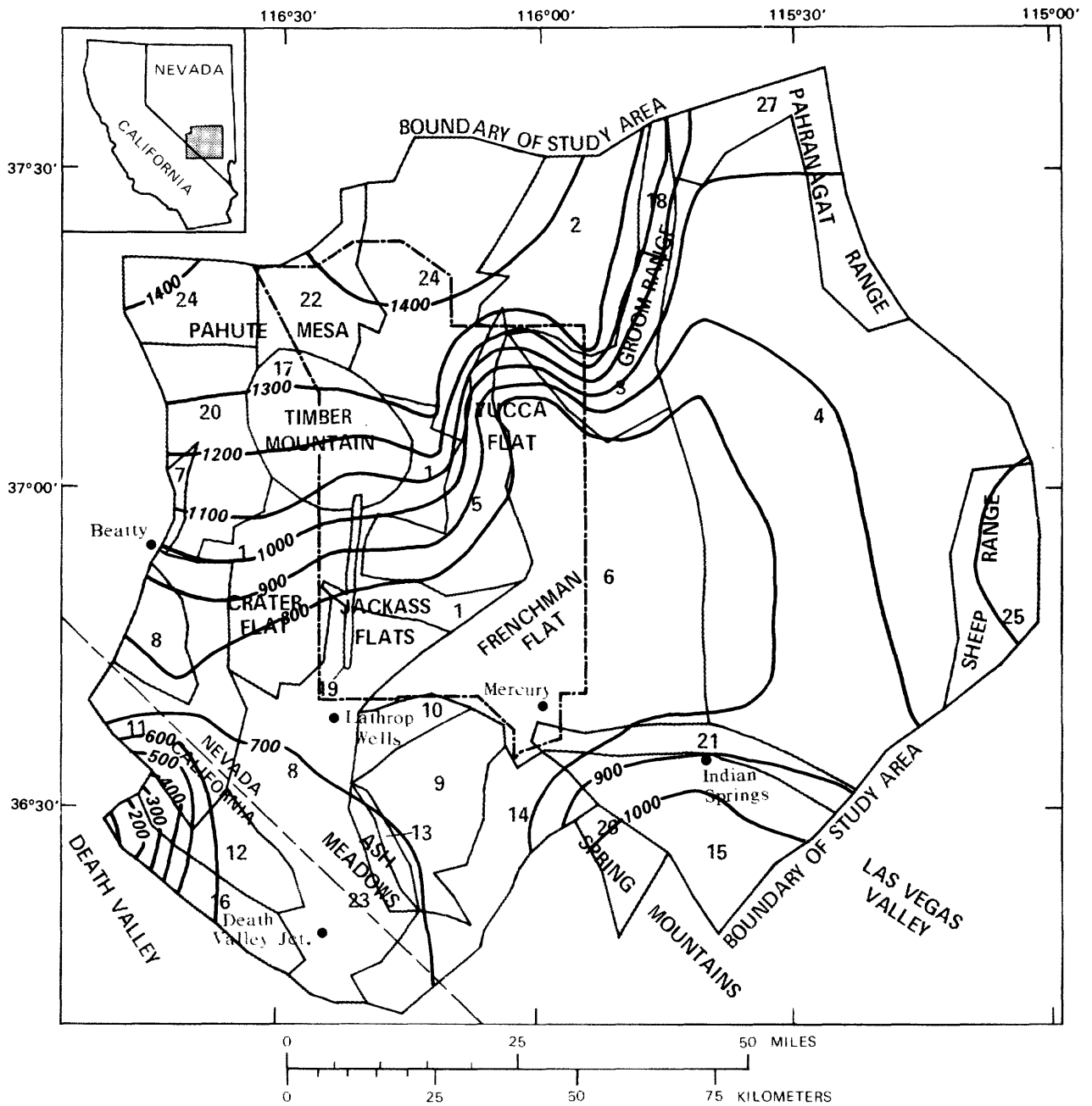
Table 2.--*Initial estimates and coefficients of variation  
of model parameters*

[Variables listed together compose one parameter.

T, transmissivity in square meters per second; Q, flux in cubic  
meters per second; number following letter is zone number;

dv, Death Valley; af, Alkali Flat]

Parameter	Initial estimates	Coefficient of variation
T1	$8.0 \times 10^{-5}$	0.25
T2	$1.2 \times 10^{-3}$	1.00
T3, T18	$4.0 \times 10^{-5}$	1.00
T4, T15, T25, T26, T27	$1.4 \times 10^{-3}$	1.00
T5	$3.0 \times 10^{-4}$	1.00
T6	$1.0 \times 10^{-1}$	.40
T7	$1.0 \times 10^{-4}$	1.00
T8	$7.5 \times 10^{-3}$	.40
T9	$5.5 \times 10^{-1}$	.50
T12	$7.0 \times 10^{-4}$	.30
T13	$1.0 \times 10^{-3}$	1.00
T16	$5.0 \times 10^{-5}$	1.00
T17	$5.0 \times 10^{-4}$	.50
T19	$1.0 \times 10^{-2}$	.20
T20	$6.0 \times 10^{-4}$	.60
T21	$3.0 \times 10^{-5}$	1.00
T22, T24	$1.2 \times 10^{-2}$	.25
Q7	$-1.2 \times 10^{-9}$	.50
Q18, Q27	$9.0 \times 10^{-11}, 4.0 \times 10^{-10}$	.30
Q24	$4.0 \times 10^{-10}$	1.00
Q25	$8.5 \times 10^{-10}$	.30
Q26	$1.0 \times 10^{-9}$	.30
Qaf	$-3.0 \times 10^{-1}$	.30
Qdv	$-1.7 \times 10^{-1}$	.20



**EXPLANATION**

- SIMULATED POTENTIOMETRIC CONTOUR**--Shows altitude of simulated potentiometric surface. Contour interval 100 meters. Datum is sea level.
- ZONE NUMBER AND BOUNDARY**
- BOUNDARY OF NEVADA TEST SITE**

Figure 3.--Simulated hydraulic heads.

inflections indicate significant changes in the direction of ground-water flow. Because isotropy has been assumed, water is assumed to flow perpendicularly to potentiometric contours. An area of small flux occurs where the angle of inflection is acute and the contours vee downgradient.

## Discussion

### Sources of Error

Nonzero residuals between simulated and measured hydraulic heads have two sources: (1) Errors in head measurement and location of wells and springs where head measurements are taken; and (2) errors due to model simulation. The first of these sources was discussed in a previous section and probably is not a significant source of error.

Error due to model simulation may have two sources. The first is caused by using a finite-element approximation of the flow equation. These inaccuracies are caused by round-off errors and by attempting to simulate smooth curves by planar surfaces. Simulations were done on a computer with approximately 14-decimal-digit accuracy; therefore, round-off error is not considered a problem. Finite-element approximation is least accurate where hydraulic gradients vary greatly (the second spatial derivative of head is greatly different from zero), and where node density is sparse. The finite-element mesh was designed to minimize this type of error; this mesh contains 685 nodes, with the node density greatest in those areas of greatest interest. The finite-element approximation may be a source of some errors, but they probably are not significant compared to those caused by the remaining source.

The second source of error in the simulation probably is the use of: (1) A two-dimensional model to simulate three-dimensional flow; (2) inaccurate zonal boundaries; (3) simplification of zonation; (4) assumption of steady-state conditions; (5) errors in distribution and rates of recharge, discharge, and leakance; and (6) inappropriate boundary conditions. The calibration process involves analysis and redefinition of the conceptual model, a step equally important as determination of model parameters. An advantage of using formalized inverse procedures is that they allow the modeler to expend efforts on improving the conceptual model rather than on changing values of variables.

Still, almost all mismatch between measured and simulated heads probably is due to uncertainty in the conceptual model.

### Distribution of Residuals

Calibration of the model involved attempts to minimize differences between measured and simulated heads (residuals) throughout the study area, while insuring that values of model parameters were realistic. The residuals range from -61.0 to +85.2 m (pl. 1). Generally, absolute values of the residuals are less than 30 m.

Two areas where residuals remain large are Pahute Mesa and Jackass Flats. Pahute Mesa is an area well-known hydrologically (Blankennagel and Weir, 1973). Extensive drilling and testing showed that transmissivity variations in Pahute Mesa are systematic but complex. In addition, measurements of head with depth in boreholes in Pahute Mesa show both upward and downward flow in different parts of the mesa. The mesh was not designed to include details of known hydrology of this area; therefore, the model is unable to simulate accurately the heads there.

Several attempts were made to decrease large residuals in Jackass Flats by altering zonal boundaries near Timber Mountain and Yucca Mountain. No subsurface data were available between the northern part of the Timber Mountain moat and the wells in Yucca Mountain and Calico Hills; therefore, these attempts were not successful.

### Measures of Fit of Simulated with Measured Hydraulic Heads

Several measures of fit were used to determine whether simulated results agreed with measurements. These include error variance,  $s^2$  (defined previously); ratio  $s/h$  (where  $h$  is the difference between largest and smallest values of measured head); and correlation between the weighted simulated and measured heads. Error variance was  $461.0 \text{ m}^2$  (square meters), resulting in a standard error of 21.5 m. In general,  $s/h$  should be small (Cooley, 1977, p. 322); ratio  $s/h$  was 0.015. Thus, although an individual residual may be large (almost 85 m in one case), overall agreement between measured and simulated heads is good. If the two largest residuals (Pahute Mesa area) were

decreased from their present values of 85.2 m and 80.5 to 50 m, error variance would be reduced to about 374 m<sup>2</sup>, and s/h would be 0.013, which is only a minor improvement.

Correlation between  $w_{\ell}^{1/2} h_{\ell}$  and  $w_{\ell}^{1/2} h_{\ell}^{obs}$  is given by:

$$R = \left\{ \frac{[\sum_{\ell=1}^J (w_{\ell}^{1/2} h_{\ell}^{obs} - \bar{h}^{obs})(w_{\ell}^{1/2} h_{\ell} - \bar{h})]^2}{\sum_{\ell=1}^J (w_{\ell}^{1/2} \bar{h}^{obs})^2 \sum_{\ell=1}^J (w_{\ell}^{1/2} h_{\ell} - \bar{h})^2} \right\}^{1/2} \quad (2)$$

where overbars indicate averages of weighted variables  $w_{\ell}^{1/2}$  and  $w_{\ell}^{1/2} h_{\ell}^{obs}$ , and the summation convention has been suspended (Cooley, 1977, p. 322).

Correlation coefficient, R, was 0.998 in this study, indicating a good fit.

### Values of Parameters

#### Description

Values of variables used in simulation, and estimates of standard errors for parameters are listed in table 3. Standard errors were calculated by the inverse procedure; they are a function of sensitivities of simulated head to changes in parameters, and the error variance, s<sup>2</sup> (Cooley, 1979, p. 606). Standard errors of parameters are measures of the range throughout which parameters may be varied without greatly changing simulated head distribution, if remaining parameters also are allowed to vary.

### Transmissivities

Zones can be grouped according to dominant lithology (carbonate, tuffaceous, clastic, or alluvial) within the zone. The carbonate rocks generally have a transmissivity three to four times that of the tuffs, and approximately two orders of magnitude greater than the Precambrian and Cambrian quartzites. The Eleana Formation has a transmissivity approximately the same as that of the clastic rocks. Transmissivity of zone 8 (predominantly alluvium) is slightly larger than average transmissivity of the carbonate rocks, but significantly less than the largest values for the carbonate rocks.

Because transmissivities range over several orders of magnitude, arithmetic means would be determined primarily by larger values; therefore,

geometric means are more appropriate measures of transmissivities of different lithologic groups than arithmetic means are. Geometric means discussed hereafter are applicable only for contrasting transmissivities of different groups; no weighting on size of the zones has been performed.

Carbonate Rocks.--Carbonate rocks have the largest transmissivities (geometric mean of  $2.2 \times 10^{-3} \text{ m}^2/\text{s}$ ) and also the largest range in transmissivities. The greater range is, in part, due to inclusion of relatively small transmissivities for zone 21, which represents the Las Vegas Valley shear zone.

Zone 9 has the largest transmissivity of all zones. Winograd and Thordarson (1975, p. 72-73) discuss several possible reasons for the high transmissivity of carbonate rocks beneath the Specter Range and beneath Amargosa Flat. These reasons include probable greater thickness of the carbonate rocks here than elsewhere; intense fracturing caused by movement along the Las Vegas shear zone, by convergence of the axes of the Spotted Range syncline and the Pintwater Range anticline, or by intersection of the shear zone and the folds; fracturing associated with the possible presence of the Specter Range thrust fault beneath Amargosa Flat, and the possible presence of solution channels.

Transmissivity of zone 12 is less than most other zones of carbonate lithology. Carbonate rocks crop out on the surface at the southeastern end of the Funeral Range, but subsurface lithology is unknown. Clastic rocks of Precambrian and Cambrian age crop out to the northwest and may be present beneath carbonate rocks exposed on the surface. Transmissivity calculated for this zone is intermediate between transmissivities typical of carbonate rocks and those of clastic units, suggesting that zone 12 may be a mixture of lithologies from these two groups. Another explanation, offered by I. J. Winograd (U.S. Geological Survey, written commun., 1981), is that the large gradient observed between the Amargosa Desert northwest of the Funeral Range and the springs near Furnace Creek Ranch might be caused by a fault zone of lower transmissivity than the carbonate rocks it penetrates. Transmissivity determined for zone 12 then would be representative of the fault zone rather than carbonate rocks.

Table 3.--Values of model variables and standard errors

[Variables listed together compose one parameter.

T, transmissivity, in square meters per second, Q, flux, in cubic meters per second; number following letter is zone number; dv, Death Valley; af, Alkali Flats; pr, Pahrnagat Range; rs, Resting Springs Range, chd, constant head node. Standard errors not estimated for parameters held constant and for Qchd]

Model variable	Value	Standard error	Coefficient of variation
T1	$7.707 \times 10^{-5}$	$1.948 \times 10^{-5}$	0.253
T2	$2.341 \times 10^{-3}$	$9.716 \times 10^{-4}$	.415
T3, T18	$4.671 \times 10^{-5}$	$9.996 \times 10^{-6}$	.214
T4, T15, T25, T26, T27	$1.388 \times 10^{-3}$	$3.179 \times 10^{-4}$	.229
T5	$2.190 \times 10^{-5}$	$8.861 \times 10^{-6}$	.405
T6	$9.438 \times 10^{-2}$	$3.259 \times 10^{-2}$	.345
T7	$3.114 \times 10^{-4}$	$3.386 \times 10^{-4}$	1.087
T8	$8.616 \times 10^{-3}$	$2.005 \times 10^{-3}$	.238
T9	$5.573 \times 10^{-1}$	$2.716 \times 10^{-1}$	.487
T10, T11, T14	$6.192 \times 10^{-5}$	--	--
T12	$6.780 \times 10^{-4}$	$1.393 \times 10^{-4}$	.205
T13	$1.084 \times 10^{-3}$	$3.625 \times 10^{-4}$	.334
T16	$6.257 \times 10^{-5}$	$8.627 \times 10^{-6}$	.164
T17	$4.731 \times 10^{-4}$	$1.514 \times 10^{-4}$	.320
T19	$1.090 \times 10^{-2}$	$1.916 \times 10^{-3}$	.084
T20	$7.494 \times 10^{-4}$	$1.773 \times 10^{-4}$	.237

Table 3.--Values of model variables and standard errors--Continued

Model variable	Value	Standard error	Coefficient of variation
T21	$3.586 \times 10^{-5}$	$1.712 \times 10^{-5}$	0.477
T22, T24	$9.420 \times 10^{-4}$	$1.929 \times 10^{-4}$	.205
T23	$3.000 \times 10^{-5}$	--	--
Q7	$-4.847 \times 10^{-2}$	$-1.747 \times 10^{-2}$	.358
Q13	$-6.653 \times 10^{-1}$	--	--
Q18	$1.154 \times 10^{-2}$	$3.188 \times 10^{-3}$	.275
Q24	$5.351 \times 10^{-1}$	$7.260 \times 10^{-2}$	.152
Q25	$4.164 \times 10^{-1}$	$8.702 \times 10^{-2}$	.209
Q26	$1.866 \times 10^{-1}$	$3.882 \times 10^{-2}$	.208
Q27	$1.851 \times 10^{-1}$	$5.111 \times 10^{-2}$	.275
Qaf	$-2.962 \times 10^{-1}$	$-8.838 \times 10^{-2}$	.298
Qchd	$-1.858 \times 10^{-1}$	--	--
Qdv	$-1.697 \times 10^{-1}$	$-2.418 \times 10^{-2}$	.142
Qrs	$1.122 \times 10^{-2}$	--	--
Qpr	$1.950 \times 10^{-2}$	--	--

Tuffs.--The geometric mean of transmissivities of zones composed predominantly of tuffs is about  $5.6 \times 10^{-4} \text{ m}^2/\text{s}$ . Hydraulic conductivity of tuffaceous rocks at the test site is determined largely by the number and properties of fractures (Blankennagel and Weir, 1973), and is, therefore, a function of mode of emplacement, degree of welding, structural setting, and extent of filling of fractures by secondary minerals. Because of the complexity of stratigraphy and structure within tuffaceous rocks, hydraulic conductivities may vary greatly within short distances. Values listed are representative of averages of transmissivities of large volumes of rock, and may be greatly different from values determined by borehole techniques.

Zone 19 has a transmissivity significantly larger than the geometric mean. This zone, representing the Fortymile Canyon fracture system, was determined to have a value of about  $1 \times 10^{-2} \text{ m}^2/\text{s}$ . Evidence for the large transmissivity of this zone includes large values of transmissivity observed in two wells within the zone, and veeing of potentiometric contours up Fortymile Canyon. Veeing of the contours indicates that flow of ground water beneath northern Yucca Mountain is southeast toward Fortymile Wash.

Clastic Rocks and Argillite.--The geometric mean of transmissivities for the clastic units is about  $5.4 \times 10^{-5} \text{ m}^2/\text{s}$ . Transmissivities were determined from a few aquifer tests and the inverse procedure. Transmissivity of the Eleana Formation, determined by the inverse procedure, is  $2.2 \times 10^{-5} \text{ m}^2/\text{s}$ . Aquifer-test information for several wells in the Eleana in Syncline Ridge west of Yucca Flat indicates that transmissivities range from  $6 \times 10^{-7}$  to about  $7 \times 10^{-4} \text{ m}^2/\text{s}$  (Dinwiddie and Weir, 1979). Larger transmissivities obtained from aquifer-test data may be the result of fractures of local extent; these transmissivities may not be representative of overall transmissivity of the zone.

Transmissivity of zone 16, which represents the Furnace Creek fault zone, is of the same order as transmissivities of the clastic units and is less than transmissivities of tuffs. No hydrologic testing data are available for zone 16. This zone has a smaller transmissivity than rocks immediately upgradient from it, especially in the vicinity of Furnace Creek Ranch, as indicated by the presence of springs along its upgradient boundary.

Rocks beneath the Amargosa Desert.--Zone 8 represents a combination of lithologies, including limestones and dolomites, tuffaceous rocks, lakebeds, and gravel. Overall transmissivity of this zone, as suggested by the model, is approximately the same as some of the carbonate units. It is greater than regional transmissivities for the tuffs, suggesting that tuffs may not play an important role in the zone. Isopachous maps of tuffs associated with the eruption of Timber Mountain (Byers and others, 1968) indicate that the zero isopach line is near the southern boundary of the test site. Aeromagnetic data (Greenhaus and Zablocki, 1982) indicate that strongly magnetized tuffs are not present in significant amounts beneath the Amargosa Desert. These data and geologic mapping indicate that magnetized tuffs are present south of the Furnace Creek Ranch fault zone. Bedded and reworked tuffs are present along margins of the Amargosa Desert south of Ash Meadows and east of the Funeral Range (Denny and Drewes, 1965). Alluvium is an important medium for ground-water flow beneath parts of the Amargosa Desert. Geochemical evidence and drillers' logs indicate that the Fortymile Wash alluvial system controls flow west and southwest of Lathrop Wells (A. F. White, U.S. Geological Survey, oral commun., 1979). Major transmissive units to the south are unknown, but they probably include limestones and dolomites.

#### Fluxes

Based on absolute values, principal flux terms are discharge at Ash Meadows, recharge/underflow in Pahute Mesa, recharge in the Sheep Range and Spring Mountains, and discharge at Alkali Flat. Because of the lack of potentiometric data in the easternmost part of the area, the inverse technique was unable to test Winograd and Friedman's (1969) hypothesis that 35 percent of the discharge at Ash Meadows is derived from Pahrnatagat Valley. Assuming that their hypothesis is correct, estimates for recharge occurring beneath the Sheep Range (zone 25) and the Pahrnatagat Range (zone 27) are too large. The flux across the Resting Springs Range from Pahrump Valley is a very minor part of the discharge at Alkali Flat.

## Standard Errors

Standard errors in parameters were estimated by the inverse procedure (Cooley, 1979, p. 606; R. L. Cooley, U.S. Geological Survey, written commun., 1981). Uncertainty in the parameters normally is larger than that indicated by estimated standard error. As stated by Cooley (1979, p. 606) "Standard errors \*\*\* are measures of the ranges over which the respective parameters may be varied and produce a similar solution for the head distribution as that obtained by using  $\hat{a}$  [the value of the parameter]."

Standard errors range from 8.4 to 108.7 percent of the associated parameter values (table 3); about one-half of the coefficients of variation (error divided by value) are between 20 and 30 percent. Parameters with the smallest coefficients of variation are transmissivities of zone 19 (tuffs beneath Fortymile Canyon) and zone 16 (tuffs and lakebeds along Furnace Creek Wash), recharge on and underflow beneath Pahute Mesa (Q24), and discharge at Death Valley (Qdv). The most poorly determined parameters are transmissivities of zone 7 (tuffs in Oasis Valley, where the estimated error exceeds value of parameter); zone 2 (tuffs beneath the Belted Range and alluvium beneath western Emigrant Valley); zone 5 (Eleana Formation); zone 9 (carbonate rocks beneath Amargosa Flat); and zone 21 (carbonate rocks and fault gouge along the Las Vegas Valley shear zone).

The degree of uncertainty probably is larger than indicated. The variable for discharge at Ash Meadows was held constant, but probably contains 10 to 20 percent error. Because an important variable must be held constant to make the problem soluble, it was not possible to include this estimated error in the simulations and subsequent error analysis; therefore, the estimated errors for other parameters are probably too small.

Estimated standard errors discussed previously present a pessimistic view, if they are considered only in terms of their magnitudes. However, overall range in transmissivities is greater than four orders of magnitude, and the area is very complex geologically. In spite of the degree of uncertainty in values of parameters and the complexity of the area, the fit between measured and simulated potentials generally is quite good. Several problem areas do exist, but further refinement of the model for these areas is not possible without additional data.

The model is not unique; other combinations of zones representing different conceptual models could result in similar solutions and matches to the measured heads. Certain aspects of any conceptual model would not be different. Presence of the barriers and large transmissivity of the carbonates are well-documented. Correlation between altitude and precipitation is well-established, even though correlation between altitude and recharge is tenuous. Locations of discharge points are well-known; measurements of discharge generally are good. Models probably would differ in locations of zones and zonal boundaries, and locations of outer boundaries of the model. Because of known constraints on the system, any type of model probably would yield similar results.

#### Calculated Fluxes

One of the prime reasons for modeling ground-water flow near the Nevada Test Site is to predict movement of radionuclides from a repository. These predictions can be done only through transport modeling, which requires estimates of flux. The flow model provides these flux estimates; some results are given in table 4. Flux is expressed as a unit flux (the flux through a cross section of the aquifer 1 m wide). Twelve sites in the western part of the study area were chosen for calculation of fluxes; these sites (A-L) extend from near Beatty to Death Valley (pl. 1). Calculated fluxes range from approximately  $4.4 \times 10^{-7} \text{ m}^2/\text{s}$  to  $8.8 \times 10^{-5} \text{ m}^2/\text{s}$ . Units with smallest fluxes are those with smallest transmissivities, namely the Eleana Formation and the tuffs represented in zone 1. The greatest flux is in the carbonate aquifer beneath Amargosa Flat (zone 9). Other large fluxes occur in zones 8 and 12.

#### SENSITIVITY ANALYSES

Sensitivity analyses were performed to determine the effects of uncertainties in parameters on model calculations. These analyses serve two purposes:

1. Estimates may be made of errors in the output of the model. Because this model will be used to calculate fluxes for use as boundary conditions for a transport model of a part of the study area, uncertainty in these boundary fluxes needs to be evaluated when transport model results are evaluated.

Table 4.--Gradient, transmissivity, and unit-flux calculations for sites pertinent to a hypothetical repository located in the southwest quadrant of the Nevada Test Site

[m<sup>2</sup>/s = square meters per second]

Site	Gradient	Transmissivity (m <sup>2</sup> /s)	Unit flux (m <sup>2</sup> /s)
A	4.97 x 10 <sup>-3</sup>	7.49 x 10 <sup>-4</sup>	3.72 x 10 <sup>-6</sup>
B	2.00 x 10 <sup>-2</sup>	2.19 x 10 <sup>-5</sup>	4.38 x 10 <sup>-7</sup>
C	3.03 x 10 <sup>-2</sup>	7.71 x 10 <sup>-5</sup>	2.33 x 10 <sup>-6</sup>
D	1.02 x 10 <sup>-2</sup>	2.19 x 10 <sup>-5</sup>	2.22 x 10 <sup>-7</sup>
E	6.30 x 10 <sup>-3</sup>	7.71 x 10 <sup>-5</sup>	4.85 x 10 <sup>-7</sup>
F	9.29 x 10 <sup>-3</sup>	7.71 x 10 <sup>-5</sup>	7.16 x 10 <sup>-7</sup>
G	8.30 x 10 <sup>-4</sup>	8.62 x 10 <sup>-3</sup>	7.15 x 10 <sup>-6</sup>
H	2.09 x 10 <sup>-4</sup>	9.44 x 10 <sup>-2</sup>	1.97 x 10 <sup>-5</sup>
I	1.26 x 10 <sup>-3</sup>	8.62 x 10 <sup>-3</sup>	1.08 x 10 <sup>-5</sup>
J	1.59 x 10 <sup>-4</sup>	5.57 x 10 <sup>-1</sup>	8.83 x 10 <sup>-5</sup>
K	1.30 x 10 <sup>-2</sup>	6.78 x 10 <sup>-4</sup>	8.81 x 10 <sup>-6</sup>
L	1.99 x 10 <sup>-3</sup>	8.62 x 10 <sup>-3</sup>	1.72 x 10 <sup>-5</sup>

2. These analyses yield information on which parameters need to be better determined to improve reliability of model results.

### Hydraulic-Head Analysis

#### Procedure

Evaluation of the effects of uncertainty in model parameters is best done through a formalized procedure. The inverse procedure used in this study requires computation of a scaled-sensitivity matrix with elements  $S_{jk}$ , where the subscript  $j$  represents node number, and the subscript  $k$  represents parameter number (Cooley, 1977, p. 319-320). As the algorithm converges,

$$\frac{\partial h_j}{\partial a_k} = \frac{S_{jk}}{a(k)}, \quad (5)$$

where parentheses indicate no summation is to be performed, and  $a$  is parameter value. These values are the desired sensitivities.

The value of:

$$(dh_j)_k = \frac{\partial h_j}{\partial a_k} da_k = S_{jk} \frac{da_k}{a_k}$$

is the change in  $h_j$  that would result with small changes in  $a_k$ . Because the solution for hydraulic head is nonlinear with respect to  $a_k$ , large changes in any of the  $a_k$  could result in very different results than the above expression would predict.

Comparison of sensitivities is difficult because of the wide range in values of model parameters. Ignoring problems of nonlinearity, sensitivity is the amount of head change that would occur if  $da_k$  were equal to 1. The proportion of change in  $a_k$  (expressed as  $da_k/a_k$ ) equals  $1/a_k$ ; therefore, it varies greatly among the  $a_k$ . The new value of the parameter ( $da_k + a_k$ ) equals  $1 + a_k$ , and may be very unrealistic for parameters much smaller than 1. Scaled sensitivity ( $S_{jk}$ ) is the amount of head change occurring when  $da_k$  equals  $a_k$ ; the proportion of change equals 1 and is the same for all  $a_k$ . The new value of the parameter would be  $da_k + a_k$  equals  $2a_k$ , which is reasonable. Therefore, scaled sensitivities are useful for comparing sensitivity of the model to different parameters.

Several characteristics of sensitivities may be determined by considering the expression for steady-state distribution of head for one-dimensional flow in a homogeneous medium:

$$h = -\frac{q}{T} x + h_0 \quad (6)$$

where

$q$  = discharge,

$T$  = transmissivity,

$x$  = space coordinate, and

$h = h_0$ , at  $x = 0$ .

The scaled sensitivities to  $T$  and  $q$  are:

$$a_k \frac{\partial h}{\partial a_k} \bigg|_{a_k=T} = T \frac{\partial h}{\partial T} = \frac{q}{T} x = -\frac{\partial h}{\partial x} x \quad (7)$$

and

$$a_k \frac{\partial h}{\partial a_k} \bigg|_{a_k=q} = q \frac{\partial h}{\partial q} = -\frac{q}{T} x = \frac{\partial h}{\partial x} x, \quad (8)$$

and the ratio of scaled sensitivities is

$$\frac{T \frac{\partial h}{\partial T}}{q \frac{\partial h}{\partial q}} = -1. \quad (9)$$

While this example is too simple to describe realistically interactions in a two-dimensional, non-homogeneous model with distributed fluxes, it is useful to make some general observations:

1. Scaled sensitivity with respect to both discharge and transmissivity increases as distance from the point of constant head increases (moment effect).
2. Absolute values of scaled sensitivities with respect to transmissivity and flux decrease as transmissivity increases.
3. Scaled sensitivities with respect to both types of parameters are functions of flux.
4. Magnitudes of the sensitivities are equal, but the sensitivities are opposite in sign.

These points are true only for the one-dimensional, homogeneous model described, but provide a framework to interpret more complex models.

### Results and Discussion

A summary of the scaled head sensitivities for all nodes is presented in table 5. Values of minimum and maximum sensitivities of each parameter and the sum of absolute values of the scaled sensitivities are included in this table. Minimum and maximum values give an indication of the sensitivity of individual nodes to variations in a parameter, while the sum of absolute values gives an indication of the sensitivity of the entire model. Using the sum of absolute values performs a weighting based on the distribution of nodes within the study area; therefore, it increases the importance of sensitivities of nodes in the western part of the area.

Ranking sums of absolute values provides a convenient way to compare sensitivities, and results in the following partial list: Q24, Q25, T8, (T3, T18), (Q18, Q27), (T4, T15, T25, T26, T27), Q26, Qdv, T17, Q7, T19, T5, and T1. [The parentheses indicate variables that were grouped together as single parameters. The group (T4, T15, T25, T26, T27) hereafter will be referred to as (T4...)]. Although Q18 and Q27 have different values, they are treated as a single parameter; the ratio between the two variables was held constant (as discussed above). Only parameters with a sum of absolute values exceeding  $1 \times 10^4$  m were included in the list.] Six of the 8 flux parameters are in the list; only 7 of the 17 transmissivity parameters are in the list, indicating that the model is more sensitive to flux parameters.

Considering only flux parameters for the moment, comparison of the ranking of sensitivities with the ranking of absolute values of the flux parameters yields information on the model. Ranking of the sensitivities gives:

Q24, Q25, (Q18, Q27), Q26, Qdv, Q7, and Qaf;

while, ranking of magnitude of parameters (table 3) gives:

Q24, Q25, Qaf, (Q18, Q27), Q26, Qdv, and Q7.

The ranking is approximately the same in both lists, except for the position of Qaf. Sensitivity of the model to flux parameters is proportional to the

Table 5.--Summary of scaled hydraulic-head sensitivities

[Variables listed together compose one parameter; T, transmissivity; Q, flux; number following letter is zone number; dv, Death Valley; af, Alkali Flat; ug, upgradient; dg, downgradient; signs in parentheses indicate sign of sensitivity of indicated areas]

Parameter	Scaled sensitivities (meters)			Sum of absolute values	Area of maximum influence
	Minimum	Maximum	Maximum		
T1	-69.9	59.9	1.05 x 10 <sup>4</sup>	Pahute Mesa (-)	
T2	-27.4	36.1	3.92 x 10 <sup>3</sup>	East of Groom Range (+), Pahute Mesa (-)	
T3, T18	-255.6	17.5	3.86 x 10 <sup>4</sup>	West of Groom Range (-)	
T4, T15, T25, T26,	-332.8	.5	3.44 x 10 <sup>4</sup>	Sheep Range, Timpahute Range (-)	
T27					
T5	-126.8	7.7	1.88 x 10 <sup>4</sup>	West of Yucca Flat (-)	
T6	-19.2	.3	4.88 x 10 <sup>3</sup>	East of test site, Yucca Flat (-)	
T7	-10.1	17.1	6.93 x 10 <sup>2</sup>	South end Oasis Valley (+), North end Oasis Valley (-)	
T8	-105.4	2.3	5.75 x 10 <sup>4</sup>	Everywhere ug of zone 8 (-)	
T9	-3.4	1.0	1.77 x 10 <sup>3</sup>	ug of zone 9 (-)	
T12	-2.8	344.4	5.78 x 10 <sup>3</sup>	Death Valley (+)	

Table 5.--Summary of scaled hydraulic-head sensitivities--Continued

Parameter	Scaled sensitivities			Area of maximum influence
	Minimum	Maximum	Sum of absolute values (meters)	
T13	- .6	52.6	$4.44 \times 10^2$	Southwest of Ash Meadows (+)
T16	-1.7	318.9	$1.57 \times 10^3$	Death Valley (+)
T17	-142.5	72.1	$2.20 \times 10^4$	ug of Timber Mountain (-)
T19	-134.3	2.8	$1.90 \times 10^4$	North Fortymile Canyon (-)
T20	-113.8	121.4	$9.37 \times 10^3$	South end Oasis Valley (+), North of Oasis Valley (-)
T21	-113.8	4.30	$3.97 \times 10^3$	Spring Mountains (-)
T22, T24	-94.6	33.1	$5.99 \times 10^3$	North Pahute Mesa (-)
Q7	-120.2	-1.2	$1.94 \times 10^4$	Oasis Valley (-)
Q18, Q27	4.7	203.2	$3.78 \times 10^4$	Timpahute Range, Groom Range (+)
Q24	13.0	827.5	$2.10 \times 10^5$	Pahute Mesa (+)
Q25	10.0	364.2	$6.40 \times 10^4$	Sheep Range (+)
Q26	4.5	413.5	$3.32 \times 10^4$	Spring Mountain (+)
Qaf	-14.0	-8.5	$6.78 \times 10^3$	Alkali Flat (-)
Qdv	-719.0	-4.1	$2.61 \times 10^4$	Death Valley (-)

magnitude of the parameter, as indicated by analysis of the one-dimensional, homogeneous model. The anomalous behavior of Qaf can be explained: The constant head node is located in Alkali Flat; for the hydraulic head at the node to be constant, flux either in or out of the node must occur. With flux-parameter values determined by the inverse procedure, this flux is approximately  $-0.186 \text{ m}^3/\text{s}$  (discharge). Because of mass-balance constraints, if one flux parameter is varied, implicit flux at the constant head node also must vary in the opposite direction. Therefore, changes in Qaf are countered by changes in implicit discharge at the constant head node; resulting changes in simulated heads are small.

The influence of Q24 may be seen by noting the similarity between contours of sums of absolute values of sensitivity with respect to Q24 in figure 4, and simulated isopotentials shown in figure 3. Differences between the two maps occur where other flux terms are important, such as the Sheep Range, Spring Mountains, and Death Valley. Areas most sensitive to these three parameters are areas where these respective fluxes occur.

The transmissivity term that the model is most sensitive to is T8, although heads at individual nodes are not very sensitive to changes in T8. Gradients within the zone are relatively small, so that, using the one-dimensional, homogeneous model as a guide, sensitivity of simulated heads to changes in T8 also should be small; ranking absolute values of maximum and minimum scaled sensitivities places T8 in 10th position. Zone 8 represents most of the Amargosa Desert, which receives underflow from both the Oasis Valley and Ash Meadows ground-water basins, and from the area north of Jackass Flats. The constant head node is located in the southern (and downgradient) part of the zone. If T8 is decreased, heads near the upgradient end of the zone increase. Heads at all nodes upgradient from the zone also must increase. Because the zone is near the end of the flow system, heads throughout most of the modeled area are affected; the result is a large total sensitivity, even though the greatest change for any node is not large.

Change in the transmissivity parameter (T3, T18) has the next greatest effect on the model. Zones 3 and 18 represent clastic rocks beneath the Groom Range. A large potentiometric gradient exists across the zones, indicating that sensitivities to changes in the parameter may be large. Heads of nodes

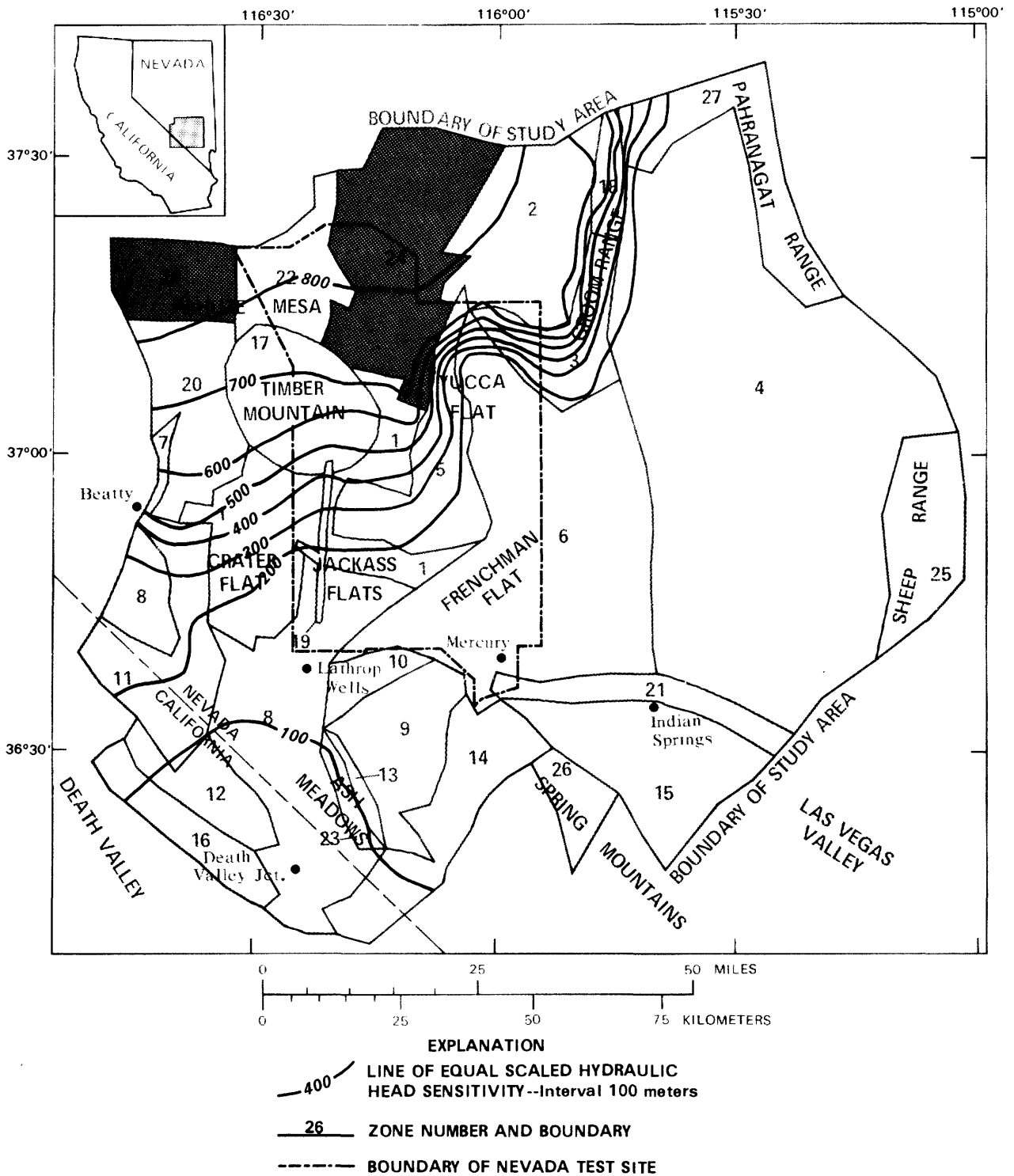


Figure 4.--Scaled hydraulic-head sensitivities with respect to the flux of zone 24.

downgradient from the zone are relatively insensitive to changes in the parameter, but heads of nodes on Pahute Mesa, Timber Mountain, and northern Jackass Flats are fairly sensitive; there, sensitivities range from about -100 to -200 m. As transmissivities of zones 3 and 18 are increased, more water flows through zones 3 and 18, and less flows through the western part of the modeled areas. The head change resulting from this redistribution of water is a function of transmissivity at a node, and the position of the node relative to zones 3 and 18. For example, immediately upgradient from the zones, transmissivity is relatively small, and sensitivities are large (-255 m). Immediately downgradient, transmissivity is large, and sensitivities are small (less than +18 m).

The sensitivity of the model to the parameter (T4...) is an example of the moment effect. Heads at the downgradient end of zone 4 are determined by transmissivities of zones downgradient, and fluxes through them. Therefore, sensitivities in downgradient zones are relatively insensitive to changes in (T4...). The gradient in zone 4 is small; sensitivity of heads within the zone also should be small. However, the zone is quite large, resulting in a significant moment effect. Nodes at the upgradient ends of the zone are moderately sensitive to changes in (T4...); scaled sensitivity at one node is -332.8 m.

T9 is a parameter to which the model is very insensitive, despite the fact that virtually all ground water in the Ash Meadows basin flows through zone 9. Transmissivity of this zone is so large and, therefore, the gradient so small, that sensitivities are very small; scaled sensitivity of greatest magnitude is only -3.4 m.

Zone 19 is the second smallest zone, yet the model is moderately sensitive to changes in T19. Fortymile Canyon was included as a separate zone because of its proximity to Yucca Mountain, a possible site for a nuclear-waste repository, and because of large transmissivities determined from aquifer tests in the zone. The zone is narrow, and oriented approximately parallel to direction of flow of water moving toward Jackass Flats. Zones 1 and 5, on either side, have small transmissivities; zone 8 at the downgradient end has a high transmissivity. Therefore, zone 19 serves as a

high transmissivity flow path for water travelling southward from Pahute Mesa. This zone allows water to bypass less transmissive rocks on either side; potentiometric contours vee upgradient as a result. The area where heads are most sensitive to changes in T9 is the northern end of the zone (fig. 5).

Transmissivity in zone 12 is the transmissivity parameter with the greatest magnitude of scaled sensitivity (not summed over all nodes). Heads at the upgradient end of the zone are constrained by the nearby constant head node; flux through the zone is large; therefore, nodes downgradient from the zone have large sensitivities to its transmissivity. The sum of absolute values for this parameter is small, indicating its effect is local. The effect of T16 is similar.

#### Summary

1. Hydraulic heads are very sensitive to changes in larger flux parameters. Changes in head occur throughout the model, but are larger in, and near, zones where flux changes occur.
2. Changes in hydraulic head, resulting from increasing transmissivity of a zone, depend on location of the node relative to the zone and the constant head node. If the node is between the zone whose transmissivity is increased, and the constant head node, the amount of head change is relatively small. If the node is on the side away from the constant head node, the amount of head change can be much greater. The larger the transmissivity is that is being increased, the smaller the amount of head change will be. Whether the head increases or decreases depends on the location of the node relative to flow paths through the zone, whose transmissivity is varied, and the location of the node relative to the constant head node.
3. Hydraulic heads of nodes near the constant head node are constrained, so head sensitivities of these nodes is small. Head sensitivity of the constant head node is zero.

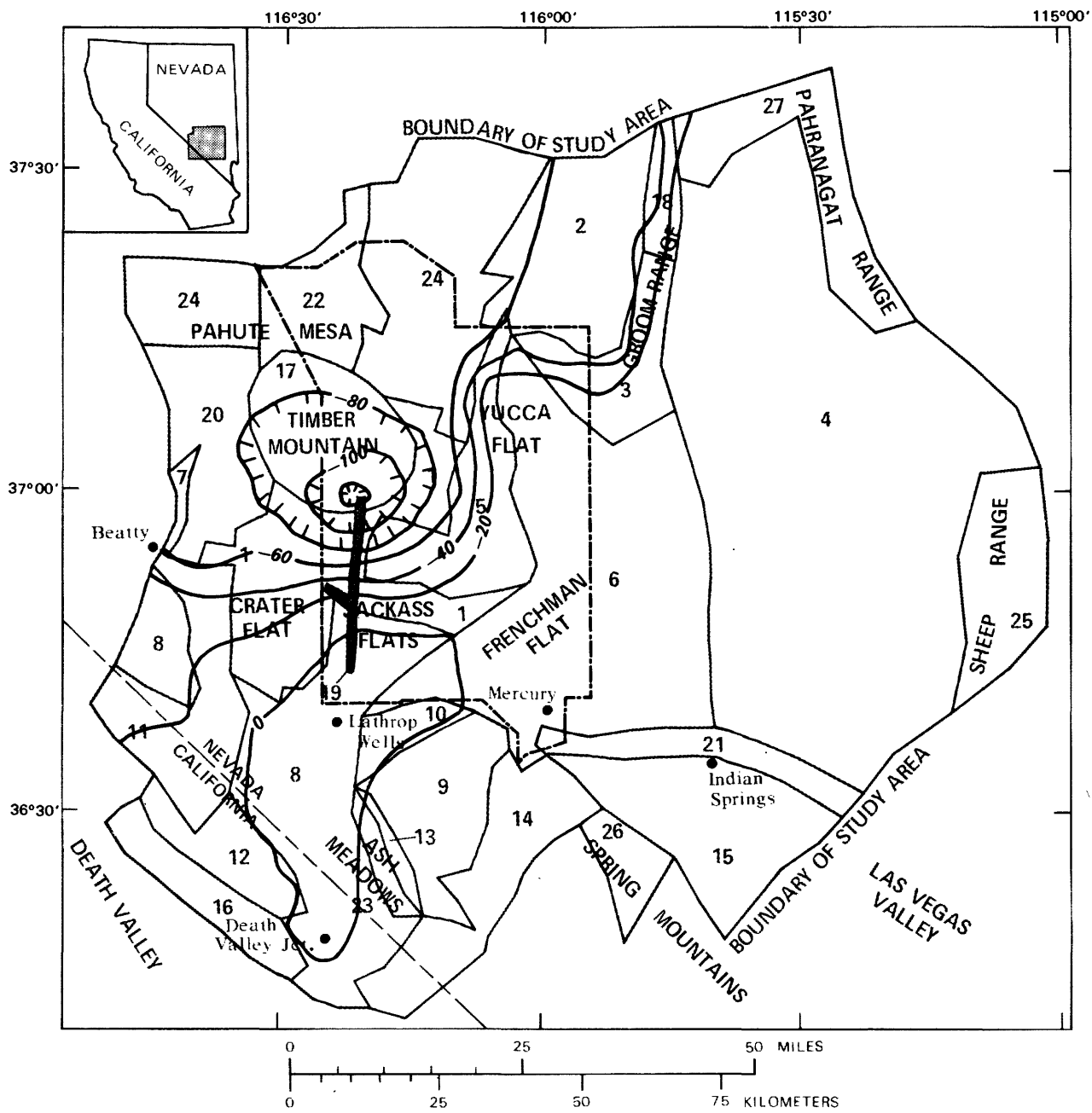


Figure 5.--Scaled hydraulic-head sensitivities with respect to the transmissivity of zone 19.

## Flux Analysis

### Procedure to Calculate Flux Sensitivity

Because isotropy has been assumed, the magnitude of the cross-sectional flux per unit length (unit flux) is:

$$Q = T \left| \text{grad } h \right| \quad (10)$$

where

T = transmissivity of the zone, and

grad h = gradient of head.

Because a finite-element approximation has been used to solve the flow equations, three nodes forming a triangle may be used to determine an approximation of the gradient. Coordinates of the three nodes may be denoted as:

$$(x_i, y_i, h_i) \quad i = 1, 2, 3$$

where

x and y = space coordinates, and

h = simulated head.

The plane intersecting the three nodes is:

$$A(x-x_1) + B(y-y_1) + C(h-h_1) = 0 \quad (11)$$

where

$$\begin{aligned} A &= (y_1 - y_2)(h_3 - h_2) - (y_3 - y_2)(h_1 - h_2), \\ B &= (x_3 - x_2)(h_1 - h_2) - (x_1 - x_2)(h_3 - h_2), \text{ and} \\ C &= (x_1 - x_2)(y_3 - y_2) - (x_3 - x_2)(y_1 - y_2). \end{aligned} \quad (12)$$

Solving for h:

$$h = -\frac{1}{C} (A(x-x_1) + B(y-y_1)) + h_1 \quad (13)$$

then

$$\text{grad } h = -\frac{1}{C} (A\hat{i} + B\hat{j})$$

and

$$|\text{grad } h| = \frac{(A^2 + B^2)^{1/2}}{|C|} \quad (14)$$

The sensitivity of Q is given by:

$$\begin{aligned}\frac{\partial Q}{\partial a_k} &= \frac{\partial T}{\partial a_k} |\text{grad } h| + T \frac{\partial}{\partial a_k} |\text{grad } h| \\ &= \frac{\partial T}{\partial a_k} \frac{(A^2+B^2)^{1/2}}{|C|} + \frac{T}{(A^2+B^2)^{1/2}|C|} \left( A \frac{\partial A}{\partial a_k} + B \frac{\partial B}{\partial a_k} \right). \quad (15)\end{aligned}$$

Evaluating the derivatives:

$$\begin{aligned}\frac{\partial A}{\partial a_k} &= \frac{\partial}{\partial a_k} [\Delta y_{12}(h_3-h_2) - \Delta y_{32}(h_1-h_2)] \\ &= \Delta y_{12} \left( \frac{\partial h_3}{\partial a_k} - \frac{\partial h_2}{\partial a_k} \right) - \Delta y_{32} \left( \frac{\partial h_1}{\partial a_k} - \frac{\partial h_2}{\partial a_k} \right) \quad (16)\end{aligned}$$

where

$$\Delta I_{ij} = I_i - I_j.$$

Similarly:

$$\frac{\partial B}{\partial a_k} = \Delta x_{32} \left( \frac{\partial h_1}{\partial a_k} - \frac{\partial h_2}{\partial a_k} \right) - \Delta x_{12} \left( \frac{\partial h_3}{\partial a_k} - \frac{\partial h_2}{\partial a_k} \right). \quad (17)$$

Substituting back into (15) and rearranging:

$$\begin{aligned}\frac{\partial Q}{\partial a_k} &= \frac{\partial T}{\partial a_k} \frac{(A^2+B^2)^{1/2}}{|C|} + \frac{T}{(A^2+B^2)^{1/2}|C|} \left[ \left( \frac{\partial h_3}{\partial a_k} - \frac{\partial h_2}{\partial a_k} \right) (A\Delta y_{12} - B\Delta x_{12}) \right. \\ &\quad \left. + \left( \frac{\partial h_1}{\partial a_k} - \frac{\partial h_2}{\partial a_k} \right) (B\Delta x_{32} - A\Delta y_{32}) \right]. \quad (18)\end{aligned}$$

The term

$$\begin{aligned}\frac{\partial T}{\partial a_k} &= 0 \text{ for } a_k \text{ not representing } T \\ &= 1 \text{ for } a_k \text{ representing } T.\end{aligned}$$

Flux sensitivity is the predicted change in flux that would occur if the model parameter,  $a_k$ , were increased in value by 1. As previously discussed, because variables have values that range over orders of magnitude, comparison of sensitivities is difficult. Sensitivities may be scaled by value of the parameter, so that sensitivities of the model to different parameters may be

compared. Additional scaling by the inverse of calculated flux gives a measure of proportion of the predicted change in flux. Therefore, scaled flux sensitivity is an estimate of the proportional change in unit flux that would occur if a parameter's value were changed to twice its old value; the new value is the old value ( $a_k$ ), plus the change in value ( $a_k$ ), or  $2 a_k$ . Scaled flux sensitivity is given by:

$$\frac{\partial Q}{\partial a_k} \frac{a_k}{Q}$$

### Results and Discussion

A summary of scaled flux sensitivities for the 12 locations in the western part of the study area for which unit fluxes were calculated (pl. 1) is given in table 6. Parameters in respective columns are ranked according to magnitudes of scaled sensitivities; flux and transmissivity parameters are ranked separately. Parameters are only included in the table if their scaled sensitivity is greater than 0.01.

A positive sensitivity to a flux parameter indicates that, as absolute value of the flux parameter increases, flux at the point also increases. For a discharge parameter, this means that, as amount of discharge is increased (parameter becomes more negative), flux at the site increases.

Understanding flux sensitivities requires recognition that important flux variables in the model include not only distributed recharges and discharges, and boundary fluxes that are explicit in the statement of the model, but also an implicit discharge at the constant head node. Therefore, derivatives with respect to explicit fluxes always include a change in implicit flux as well.

Sites G and H are close together; they would be expected to behave similarly to changes in parameters. However, calculated sensitivities indicate that this is not the case. The explanation for this lies in the direction of flow at these sites. Flow at site G is to the southeast across the boundary between zones 6 and 8. After crossing the boundary, the water flows toward the southwest, parallel to the boundary, until it again crosses the boundary, back into zone 8. This circuitous path is caused by the transmissivity contrast between the two zones. Water at site G originates on Pahute Mesa. Changes that increase flow from Pahute Mesa into Jackass Flats will, therefore,

Table 6.- Summary of flux sensitivities scaled by value of parameter and inverse flux

[Variables listed together compose one parameter; T, transmissivity; Q, flux; number following letter is for number; dv, Death Valley; af, Alkali Flat; included with T4 are T15, T25, T26, and T27.

Parameters are included only if scaled sensitivity is greater than 0.01]

A(20)		B(5)		C(1)		D(5)		E(1)		F(1)	
Parameter	Scaled sensitivity										
T1	$4.46 \times 10^{-1}$	T5	$5.49 \times 10^{-1}$	T1	$8.08 \times 10^{-1}$	T5	$5.10 \times 10^{-1}$	T1	$1.03 \times 10^0$	T1	$8.25 \times 10^{-1}$
T19	$-1.96 \times 10^{-1}$	T19	$-3.90 \times 10^{-1}$	T19	$-3.16 \times 10^{-1}$	T19	$-2.59 \times 10^{-1}$	T19	$-4.45 \times 10^{-1}$	T3, T18	$-2.63 \times 10^{-1}$
T3, T18	$-1.61 \times 10^{-1}$	T3, T18	$-2.51 \times 10^{-1}$	T3, T18	$-2.62 \times 10^{-1}$	T1	$2.55 \times 10^{-1}$	T8	$-2.90 \times 10^{-1}$	T20	$2.33 \times 10^{-1}$
T20	$-1.35 \times 10^{-1}$	T1	$2.17 \times 10^{-1}$	T5	$-1.45 \times 10^{-1}$	T3, T18	$-2.50 \times 10^{-1}$	T17	$2.67 \times 10^{-1}$	T19	$-1.97 \times 10^{-1}$
T5	$-1.02 \times 10^{-1}$	T4	$-9.25 \times 10^{-2}$	T20	$1.06 \times 10^{-1}$	T4	$-9.26 \times 10^{-2}$	T3, T18	$-2.43 \times 10^{-1}$	T5	$-1.39 \times 10^{-1}$
T4	$-5.93 \times 10^{-2}$	T17	$6.30 \times 10^{-2}$	T4	$-9.67 \times 10^{-2}$	T22, T24	$4.24 \times 10^{-2}$	T5	$-1.44 \times 10^{-1}$	T8	$-1.34 \times 10^{-1}$
T7	$-5.32 \times 10^{-2}$	T22, T24	$3.74 \times 10^{-2}$	T8	$5.20 \times 10^{-2}$	T8	$-3.94 \times 10^{-2}$	T4	$-8.91 \times 10^{-2}$	T17	$-1.11 \times 10^{-1}$
T22, T24	$3.92 \times 10^{-2}$	T2	$-2.64 \times 10^{-2}$	T17	$-3.37 \times 10^{-2}$	T17	$-3.61 \times 10^{-2}$	T22, T24	$2.94 \times 10^{-2}$	T4	$-9.72 \times 10^{-2}$
T12	$-3.59 \times 10^{-2}$	T20	$-2.61 \times 10^{-2}$	T2	$-2.79 \times 10^{-2}$	T20	$-2.91 \times 10^{-2}$	T2	$-2.56 \times 10^{-2}$	T12	$7.38 \times 10^{-2}$
T17	$2.62 \times 10^{-2}$	T8	$-1.52 \times 10^{-2}$	T22, T24	$2.45 \times 10^{-2}$	T6	$-2.80 \times 10^{-2}$	T6	$-1.89 \times 10^{-2}$	T2	$-2.81 \times 10^{-2}$
T8	$-2.01 \times 10^{-2}$	T6	$-1.32 \times 10^{-2}$	T12	$2.15 \times 10^{-2}$	T2	$-2.63 \times 10^{-2}$	T22, T24	$2.13 \times 10^{-2}$	T22, T24	$2.13 \times 10^{-2}$
T2	$-1.69 \times 10^{-2}$			T6	$-1.07 \times 10^{-2}$			T6	$-1.97 \times 10^{-2}$	T6	$-1.97 \times 10^{-2}$
Q24	$5.68 \times 10^{-1}$	Q24	$1.02 \times 10^0$	Q24	$1.14 \times 10^0$	Q24	$1.01 \times 10^0$	Q24	$1.04 \times 10^0$	Q24	$1.24 \times 10^0$
Q7	$3.07 \times 10^{-1}$	Q7	$-9.46 \times 10^{-2}$	Q7	$-1.85 \times 10^{-1}$	Q7	$-8.65 \times 10^{-2}$	Q7	$-1.17 \times 10^{-1}$	Q7	$-2.48 \times 10^{-1}$
Qdv	$6.60 \times 10^{-2}$	Q18, Q27	$5.24 \times 10^{-2}$	Q18, Q27	$5.19 \times 10^{-2}$	Q18, Q27	$5.29 \times 10^{-2}$	Q18, Q27	$5.95 \times 10^{-2}$	Qdv	$-1.05 \times 10^{-1}$
Q18, Q27	$3.99 \times 10^{-2}$	Q25	$2.42 \times 10^{-2}$	Qdv	$-3.94 \times 10^{-2}$	Q25	$2.35 \times 10^{-2}$	Q25	$4.26 \times 10^{-2}$	Q18, Q27	$7.82 \times 10^{-2}$
Q25	$2.89 \times 10^{-2}$	Qdv	$-1.26 \times 10^{-2}$	Q25	$1.95 \times 10^{-2}$	Qdv	$-1.34 \times 10^{-2}$	Qdv	$-1.09 \times 10^{-2}$	Q25	$7.46 \times 10^{-2}$
										Q26	$2.25 \times 10^{-2}$

Table 6.--Summary of flux sensitivities scaled by value of parameter and inverse flux--Continued

G(80)		H(6)		I(8)		J(9)		K(12)		L(8)	
Parameter	Scaled sensitivity										
T17	$3.56 \times 10^{-1}$	T3, T18	$1.37 \times 10^{-1}$	T8	$7.39 \times 10^{-2}$	T9	$1.88 \times 10^{-2}$	T12	$2.00 \times 10^{-1}$	T8	$5.05 \times 10^{-2}$
T3, T18	$-3.48 \times 10^{-1}$	T17	$-1.16 \times 10^{-1}$	T9	$-5.33 \times 10^{-2}$	T8	$-1.88 \times 10^{-2}$	T16	$-1.24 \times 10^{-2}$	T12	$-3.68 \times 10^{-2}$
T5	$-1.91 \times 10^{-1}$	T5	$.71 \times 10^{-2}$	T19	$3.48 \times 10^{-2}$			T20	$-1.18 \times 10^{-2}$	T9	$-1.14 \times 10^{-2}$
T4	$-1.28 \times 10^{-1}$	T19	$-7.31 \times 10^{-2}$	T17	$3.30 \times 10^{-2}$						
T19	$1.21 \times 10^{-1}$	T9	$-4.33 \times 10^{-2}$	T6	$-2.28 \times 10^{-2}$						
T1	$8.34 \times 10^{-2}$	T4	$3.68 \times 10^{-2}$	T12	$1.85 \times 10^{-2}$						
T6	$5.62 \times 10^{-2}$	T1	$-3.65 \times 10^{-2}$	T20	$-1.84 \times 10^{-2}$						
T8	$4.88 \times 10^{-2}$	T6	$2.47 \times 10^{-2}$	T1	$1.12 \times 10^{-2}$						
T22, T24	$4.18 \times 10^{-1}$	T20	$-2.36 \times 10^{-2}$								
T2	$-3.68 \times 10^{-2}$	T21	$1.99 \times 10^{-2}$								
T9	$3.56 \times 10^{-2}$	T8	$1.63 \times 10^{-2}$								
T20	$1.73 \times 10^{-2}$	T22, T24	$-1.57 \times 10^{-2}$								
T12	$1.27 \times 10^{-2}$	T2	$1.45 \times 10^{-2}$								
Q24	$1.23 \times 10^0$	Q25	$5.46 \times 10^{-1}$	Q24	$6.34 \times 10^{-1}$	Q24	$3.65 \times 10^{-1}$	Qdv	$1.01 \times 10^0$	T24	$1.20 \times 10^0$
Q7	$-1.52 \times 10^{-1}$	Q18, Q27	$2.39 \times 10^{-1}$	Q25	$4.72 \times 10^{-1}$	Q25	$3.07 \times 10^{-1}$	Q24	$-2.08 \times 10^{-2}$	Q25	$9.12 \times 10^{-1}$
Q25	$-1.49 \times 10^{-1}$	Q26	$1.86 \times 10^{-1}$	Q18, Q27	$2.24 \times 10^{-1}$	Q18, Q27	$1.44 \times 10^{-1}$	Q25	$1.63 \times 10^{-2}$	Q18, Q27	$4.31 \times 10^{-1}$
Qdv	$-8.64 \times 10^{-2}$	Q24	$1.55 \times 10^{-1}$	Q26	$2.08 \times 10^{-1}$	Q26	$1.24 \times 10^{-1}$	Qdv		Qdv	$-4.16 \times 10^{-1}$
Q26	$-7.96 \times 10^{-2}$	Qdv	$4.98 \times 10^{-2}$	Qdv	$1.76 \times 10^{-1}$	Q7	$-2.99 \times 10^{-2}$	Q7		Q7	$-1.10 \times 10^{-1}$
Q18, Q27	$-1.40 \times 10^{-2}$			Q7	$-4.97 \times 10^{-2}$	Qdv	$-2.62 \times 10^{-2}$	Qdv		Qaf	$-2.93 \times 10^{-2}$

increase flux at site G. Examples include: (1) Decreasing (T3, T18) and T5, so additional water is diverted to the west; and (2) increasing, T1, T17, and T19, so more water travels through these zones into Jackass Flats. Another way to increase flux at site G is to increase gradient at the site by lowering heads in zone 6; this can be done by increasing T6. Flux at the site is more sensitive to these changes than to changes in T8.

Scaled sensitivities for site H to transmissivity parameters are almost all of the opposite sign of sensitivities of the corresponding parameters for site G. Water at site H originates in the Ash Meadows basin, so parameters that increase flow rates in that subsystem will increase flux at site H.

At site A (in zone 20), an increase in T20 causes a decrease in flux. This is contrary to what normally would be expected, and requires that flow be diverted away from the site. The path of least resistance for flow through zone 20 is across its southern end (near Beatty), across the relatively narrow arm of a barrier (zone 11), into the western part of zone 8, across a narrow neck of zone 11, and into the eastern, larger segment of zone 8. The southern extension is rather narrow, and is southwest of site A. As transmissivity of zone 20 increases, flow through this narrow part of the zone increases. Flow lines are shifted to the west, away from site A in the eastern part of the zone, and flux at site A decreases.

Changes in T19 have large effects on fluxes throughout the Jackass Flats and Timber Mountain areas. If T19 is increased, flux through zone 19 increases. Because the transmissivity of the zone (which is not areally extensive) is much greater than surrounding zones, and because the zone is oriented approximately parallel to direction of flow, water travels through the zone in preference to surrounding zones. Therefore, increasing T19 causes a decrease in flux in zones surrounding zone 19.

Sensitivities to flux parameters, especially recharge parameters, are generally easier to interpret than transmissivity terms. Normally, as a recharge parameter is increased, fluxes throughout most of the system will increase. Increase in recharge is compensated for by an increase in discharge at the constant head node; discharge at other discharge areas remains unchanged. Because the constant head node is located near the bottom of the flow system, and because it is a discharge point, changes in its discharge will

affect the system upgradient. For example, an increase in Q24 results in higher heads throughout almost all the study area (fig. 4). Amounts of head increases are greater near the recharge area, and less farther away from it; therefore, gradient (and flux) is increased throughout most of the area. The amount of flux change depends on location within the system.

Sensitivities to discharge parameters are a little more difficult to interpret than sensitivities to recharge parameters. The interaction between discharge parameters and discharge at the constant head node means that the spatial relationship between the site and both discharge area and constant head node is important. If flow through the site is toward the discharge area whose discharge is being increased, flux through the site will increase. Conversely, if flow through the site is toward the constant head node, flux will decrease. If flow is toward another discharge area, flux may increase or decrease depending on response of the potential field.

The greatest flux parameter, Q24, is also the flux parameter to which all but two of the sites are most sensitive. As stated previously, sensitivity to variations in a flux parameter may be due to either a change in that parameter or to an accompanying change in discharge at the constant head node. Site K provides a good example; calculated sensitivity to Q24 is negative. Increase in discharge from the constant head node caused by an increase in Q24 results in a decrease in gradient and flux at site K.

Flux at site G decreases when some recharge parameters are increased. At site H, the more important flux parameters (Q25, (Q18, Q27), and Q26) are those that primarily affect the Ash Meadows basin. An increase in these parameters causes a higher head in zone 6 near site G, thereby lowering gradient and flux at site G.

A summary of flux sensitivities scaled by the standard error of the parameter and inverse flux is given in table 7; it is useful in determining which parameters contribute most to uncertainty in flux calculations. This analysis assumes that: (1) Zonation is accurate; (2) the zones are homogeneous and isotropic; (3) there is no vertical flow; (4) the system is at steady state; and (5) transient effects from drilling and pumping have dissipated and do not affect head observations. Uncertainties due to possible violations of these assumptions are not included. The reader also

Table 7.--Summary of flux sensitivities scaled by estimated standard error of parameter and inverse flux  
 [Variables listed together compose one parameter; T, transmissivity; Q, flux; number following letter is  
 for number; dv, Death Valley; af, Alkali Flat; included with T4 are T15, T25, T26, and T27.

Parameters are included only if scaled sensitivity is greater than 0.01]

Site (Zone)																	
A(20)			B(5)			C(1)			D(5)			E(1)			F(1)		
Variable	Scaled sensitivity	Variable	Scaled sensitivity	Variable	Scaled sensitivity	Variable	Scaled sensitivity	Variable	Scaled sensitivity	Variable	Scaled sensitivity	Variable	Scaled sensitivity	Variable	Scaled sensitivity	Variable	Scaled sensitivity
T1	$1.13 \times 10^{-1}$	T5	$2.22 \times 10^{-1}$	T1	$2.04 \times 10^{-1}$	T5	$2.06 \times 10^{-1}$	T1	$2.59 \times 10^{-1}$	T1	$2.08 \times 10^{-1}$						
T7	$-5.79 \times 10^{-2}$	T19	$-6.85 \times 10^{-2}$	T5	$-5.85 \times 10^{-2}$	T1	$6.44 \times 10^{-2}$	T17	$8.53 \times 10^{-2}$	T3, T18	$-5.63 \times 10^{-2}$						
T5	$-4.13 \times 10^{-2}$	T1	$5.49 \times 10^{-2}$	T3, T18	$-5.61 \times 10^{-2}$	T3, T18	$-5.35 \times 10^{-2}$	T19	$-7.82 \times 10^{-2}$	T5	$-5.62 \times 10^{-2}$						
T3, T8	$-3.46 \times 10^{-2}$	T3, T18	$-5.33 \times 10^{-2}$	T19	$-5.56 \times 10^{-2}$	T19	$-4.55 \times 10^{-2}$	T8	$-6.74 \times 10^{-2}$	T20	$5.52 \times 10^{-2}$						
T19	$-3.45 \times 10^{-2}$	T4	$-2.12 \times 10^{-2}$	T20	$2.52 \times 10^{-2}$	T4	$-2.12 \times 10^{-2}$	T5	$-5.84 \times 10^{-2}$	T17	$-3.55 \times 10^{-2}$						
T20	$-3.18 \times 10^{-2}$	T17	$2.01 \times 10^{-2}$	T4	$-2.21 \times 10^{-2}$	T17	$-1.16 \times 10^{-2}$	T3, T18	$-5.17 \times 10^{-2}$	T19	$-3.47 \times 10^{-2}$						
T4	$-1.36 \times 10^{-2}$	T2	$-1.10 \times 10^{-2}$	T8	$1.21 \times 10^{-2}$	T2	$-1.09 \times 10^{-2}$	T4	$-2.04 \times 10^{-2}$	T8	$-3.11 \times 10^{-2}$						
				T2	$-1.16 \times 10^{-2}$	T2	$-1.06 \times 10^{-2}$	T4	$-2.23 \times 10^{-2}$	T4	$-2.23 \times 10^{-2}$						
				T17	$-1.08 \times 10^{-2}$	T17	$-1.08 \times 10^{-2}$	T7	$1.73 \times 10^{-2}$	T7	$1.73 \times 10^{-2}$						
Q7	$1.08 \times 10^{-1}$	Q24	$1.39 \times 10^{-1}$	Q24	$1.55 \times 10^{-1}$	Q24	$1.37 \times 10^{-1}$	Q24	$1.41 \times 10^{-1}$	Q24	$1.68 \times 10^{-1}$						
Q24	$7.70 \times 10^{-2}$	Q7	$-3.34 \times 10^{-2}$	Q7	$-6.52 \times 10^{-2}$	Q7	$-3.05 \times 10^{-2}$	Q7	$-4.12 \times 10^{-2}$	Q7	$-8.73 \times 10^{-2}$						
Q18, Q27	$1.10 \times 10^{-2}$	Q18, Q27	$1.45 \times 10^{-2}$	Q18, Q27	$1.43 \times 10^{-2}$	Q18, Q27	$1.46 \times 10^{-2}$	Q18, Q27	$1.64 \times 10^{-2}$	Q18, Q27	$2.16 \times 10^{-2}$						
										Q25	$1.56 \times 10^{-2}$						
										Qdv	$-1.50 \times 10^{-2}$						

Table 7.--Summary of flux sensitivities scaled by estimated standard error of parameter and inverse flux--Continued

		Site (Zone)													
G(8)		H(6)			I(8)			J(9)			K(12)			L(8)	
Variable	Scaled sensitivity	Variable	Scaled sensitivity	Variable	Scaled sensitivity	Variable	Scaled sensitivity	Variable	Scaled sensitivity	Variable	Scaled sensitivity	Variable	Scaled sensitivity	Variable	Scaled sensitivity
T17	$1.14 \times 10^{-1}$	T17	$-3.73 \times 10^{-2}$	T9	$-2.60 \times 10^{-2}$	T12	$4.26 \times 10^{-2}$	T8	$1.18 \times 10^{-2}$						
T5	$-7.73 \times 10^{-2}$	T5	$3.12 \times 10^{-2}$	T8	$1.72 \times 10^{-2}$										
T3, T18	$-7.44 \times 10^{-2}$	T3, T18	$2.93 \times 10^{-2}$	T17	$1.06 \times 10^{-2}$										
T4	$-2.93 \times 10^{-2}$	T9	$-2.11 \times 10^{-2}$												
T19	$2.12 \times 10^{-2}$	T19	$-1.28 \times 10^{-2}$												
T1	$2.11 \times 10^{-2}$														
T6	$1.94 \times 10^{-2}$														
T9	$1.74 \times 10^{-2}$														
T2	$-1.53 \times 10^{-2}$														
T8	$1.14 \times 10^{-2}$														
Q2	$1.66 \times 10^{-1}$	Q25	$1.14 \times 10^{-1}$	Q25	$9.87 \times 10^{-2}$	Q25	$6.42 \times 10^{-2}$	Qdv	$1.43 \times 10^{-1}$	Q25	$1.90 \times 10^{-1}$				
Q7	$-5.35 \times 10^{-2}$	Q18, Q27	$6.61 \times 10^{-2}$	Q24	$8.60 \times 10^{-2}$	Q24	$4.95 \times 10^{-2}$	Q24		Q24	$1.62 \times 10^{-1}$				
Q25	$-3.12 \times 10^{-2}$	Q26	$3.87 \times 10^{-2}$	Q18, Q27	$6.20 \times 10^{-2}$	Q18, Q27	$3.98 \times 10^{-2}$	Q18, Q27		Q18, Q27	$1.19 \times 10^{-1}$				
Q26	$-1.66 \times 10^{-2}$	Q24	$2.10 \times 10^{-2}$	Q26	$4.33 \times 10^{-2}$	Q26	$2.58 \times 10^{-2}$	Q26		Q26	$8.48 \times 10^{-2}$				
Qdv	$-1.23 \times 10^{-2}$			Qdv	$2.51 \times 10^{-2}$	Q7	$-1.05 \times 10^{-2}$	Q7		Qdv	$-5.93 \times 10^{-2}$				
				Q7	$-1.75 \times 10^{-2}$			Q7		Q7	$-3.89 \times 10^{-2}$				

should be aware that each of the flux terms implicitly includes part of the discharge from the constant head node, and that Q13 is assumed to be known exactly, so that it will not occur in the table.

Because table 7 is derived from table 6, it would be redundant to analyze it with regard to the flow system. Because almost all standard errors of parameters were less than their associated parameter value, there are fewer parameters that met the criterion that scaled flux sensitivity be greater than 0.01. No transmissivity parameters for site J met this criterion.

For most sites, transmissivity of a site is the transmissivity term that should be better determined for more accurate calculation of flux at the site. Transmissivities for zones 3, 5, 18, and 19 are parameters that affect flux calculations throughout most of the western part of the study area; these parameters also should be better determined. Two flux parameters that should be better-known are Q24 and Q25.

#### Summary

1. Sensitivity to changes in transmissivity parameters is dependent on location in the flow field and relationship to transmissivity zones. In general, an increase in transmissivity of the zone in which the site lies will result in an increase in flux, but less than the amount of transmissivity increase. In some cases, flux decreases; this effect is attributable to complexities in the flow field caused by geometries of zones and directions of flow.
2. The transmissivity parameter that has greatest effect on flux at a site is commonly, but not always, transmissivity of the zone containing the site.
3. Transmissivity of zone 19 affects fluxes throughout the Jackass Flats and Timber Mountain areas; an increase in T19 causes decreases in calculated fluxes in nearby zones.
4. Fluxes in the Jackass Flats and Timber Mountain areas decrease if transmissivities of zones 3, 5, or 18 are increased; increased flux through these zones into the Ash Meadows basin decreases the amount of water available to flow beneath Timber Mountain and Jackass Flats.

5. Analysis of sensitivities to changes in flux parameters is complicated by accompanying changes in discharge from the constant head node.
6. For most sites considered, Q24 is the flux parameter that most affects calculated fluxes.

## CONCLUSIONS

Geology and hydrology of the Nevada Test Site and vicinity are highly complex and not entirely understood. Numerous types of rocks with different hydrologic properties, sometimes intensely structurally deformed and displaced, create a three-dimensional framework that is far from the simple, layer-cake settings for which ground-water models commonly have been developed. In this study, uncertainties exist about distribution and magnitude of transmissivity; distribution and rates of recharge, and rates of discharge; and locations of the boundaries of ground-water basins. Vertical flow, although important in some areas, has been ignored. Much of the control on distribution of transmissivity has been inferred from potentiometric data, which are poor or absent in some areas.

In spite of these difficulties, the model presented here is probably a good representation of the ground-water system in the vicinity of the test site. It certainly is not complete and totally accurate, and it does not eliminate the need for continued field studies. Many of the results derived from the model only substantiate conclusions derivable from the conceptual model presented by Winograd and Thordarson (1975). However, the model does allow the hydrologist to make his conclusions quantitative, rather than qualitative, and to estimate the error in his conclusions.

Future users of the model should ask several questions prior to trusting results from the model. First, does the model accurately describe the hydrology of the area in which they are interested? The model is not accurate in eastern Pahute Mesa; therefore, directions of flow, flow rates, and transmissivities derived from the model for this area are inaccurate. Second, were data available and adequate during development of the model to determine if the model is accurate in areas in which the user is interested? East and northeast of the test site, data are sparse. Third, do new data (available

since the model was developed) change some of the concepts on which the model is based?

Ground-water barriers within the study area have a great effect on measured, and, therefore, simulated heads. Some barriers greatly impede flow from recharge to discharge areas. Other barriers determine locations of discharge areas. Overall flux through the system is determined by amounts of recharge occurring within the area, and underflow from outside the study area. Barriers divert flow, so that flux in nearby areas containing relatively permeable rocks is increased. In particular, hydrologic properties of the Eleana Formation (zone 5) and Precambrian and Cambrian clastic rocks (zone 3) have a major effect on flux through the Timber Mountain and Jackass Flats areas.

Hydrologic properties of Fortymile Canyon and Fortymile Wash (zone 19) significantly affect calculated fluxes beneath Jackass Flats and Yucca Mountain. Because the zone is oriented parallel with flow from Pahute Mesa south into the Amargosa Desert, zone 19 has a major effect on flux in neighboring zones.

Recharge on Pahute Mesa and underflow from regions north of the mesa (Q24) have a significant impact on the model. Because of the importance of this flux, it needs to be determined more accurately. The flux beneath eastern Pahute Mesa was estimated by Blankennagel and Weir (1973), but some of this water may flow toward Oasis Valley rather than beneath Timber Mountain. However, direct measurement of recharge and underflow is difficult. Flux through the Timber Mountain area perhaps can be determined by careful measurement of hydraulic heads and hydraulic conductivities throughout the area.

Hydrologic data are lacking in the eastern part of the study area. Sensitivity analyses confirm the qualitative impression (obtained from regional potentiometric and geologic maps) that hydrologic properties within the Ash Meadows subsystem are not important for determination of fluxes and head distributions within western Jackass Flats; it is not necessary to improve on the data base for the Ash Meadows system to evaluate a potential repository in western Jackass Flats or Yucca Mountain. For a repository in the eastern part of Jackass Flats, the situation is different. Better

definition of the properties within Mercury Valley, eastern Jackass Flats, and Rock Valley would be especially important.

Estimates of rates of transport of radionuclides should not be made using the regional flow model. Calculations of fluxes are sufficient for use in determining boundary conditions for more detailed transport modeling, but areal distribution of flux and velocity would be determined best by detailed modeling, performed after detailed hydrogeology is understood. The present data base is sufficient for parametric types of studies of flow within the southwestern quadrant of the test site, but this data base requires considerable additional geophysical and geohydrologic information. Data to be collected need to include determination of hydraulic conductivities or transmissivities by means of well tests, measurement of head variation with depth, and geochemical information necessary for understanding chemical mechanisms that may retard or facilitate transport of radionuclides. Because of the possible presence of high transmissivity fracture zones, exploration needs to determine properties of fractured and nonfractured areas.

#### REFERENCES CITED

- Blankennagel, R. K., and Weir, J. E., Jr., 1973, Geohydrology of the eastern part of Pahute Mesa, Nevada Test Site, Nye County, Nevada: U.S. Geological Survey Professional Paper 712-B, p. B1-B35.
- Burchfiel, B. C., and Davis, G. A., 1972, Structural framework and evolution of the southern part of the Cordilleran orogen, western United States: *American Journal of Science*, v. 272, p. 97-118.
- \_\_\_\_\_ 1975, Nature and controls of Cordilleran orogenesis, western United States--Extension of an earlier synthesis: *American Journal of Science*, v. 275-A, p. 363-396.
- Byers, F. M., Jr., Carr, W. J., Orkild, P. P., Quinlivan, W. D., and Sargent, K. A., 1976, Volcanic suites and related cauldrons of Timber Mountain-Oasis Valley Caldera Complex, southern Nevada: U.S. Geological Survey Professional Paper 919, 70 p.
- Byers, F. M., Jr., Orkild, P. P., Carr, W. J., and Quinlivan, W. D., 1968, Timber Mountain Tuff, southern Nevada, and its relation to cauldron

- subsidence, *in* Eckel, E. B., ed., Studies of geology and hydrology, Nevada Test Site: Geological Society of America Memoir 110, p. 87-97.
- Carlson, J. E., and Willden, Ronald, 1968, Transcontinental geophysical survey (35° - 39° N) geologic map from 112°W longitude to the coast of California: U.S. Geological Survey Miscellaneous Geologic Investigations Map I-532-C.
- Christiansen, R. L., and Lipman, P. W., 1972, Cenozoic volcanism and plate-tectonic evolution of the western United States, II--Late Cenozoic: Philosophical Transactions of the Royal Society of London, Series A, v. 271, p. 249-284.
- Claassen, H. C., and White, A. F., 1979, Application of geochemical kinetic data to ground-water systems--A tuffaceous rock aquifer in southern Nevada: American Chemical Society Symposium Series, Book 93, Chapter 34, p. 771-793.
- Cooley, R. L., 1977, A method of estimating parameters and assessing reliability for models of steady state groundwater flow: Water Resources Research, v. 13, no. 2, p. 318-324.
- \_\_\_\_\_ 1979, A method of estimating parameters and assessing reliability for models of steady state groundwater flow, 2--Application of statistical analysis: Water Resources Research, v. 15, no. 3, p. 603-617.
- Denny, C. S., and Drewes, Harald, 1965, Geology of the Ash Meadows quadrangle, Nevada-California: U.S. Geological Survey Bulletin 1181-L, p. L1-L56.
- Dickinson, W. R., 1977, Paleozoic plate tectonics and the evolution of the Cordilleran continental margin, *in* Stewart, J. H., Stevens, C. H., and Fritsche, A. E., eds., Paleozoic paleogeography of the western United States: Pacific Coast Paleogeography Symposium, 1st, Bakersfield, California, 1977, Proceedings: Bakersfield, California, Society of Economic Paleontologists and Mineralogists, Pacific Section, p. 137-155.
- Dinwiddie, G. A., and Weir, J. E., Jr., 1979, Summary of hydraulic tests and hydrologic data for holes UE16d and UE16f, Syncline Ridge area, Nevada Test Site: U.S. Geological Survey Report 1543-3, 25 p.
- Dudley, W. W., Jr., and Larson, J. D., 1974, Geologic controls on spring locations, Ash Meadows, Nye County, Nevada [abs.]: Geological Society of America Abstracts with Programs, v. 6, no. 3, p. 167.

- \_\_\_\_\_ 1976, Effect of irrigation pumping on desert pupfish habitats in Ash Meadows, Nye County, Nevada: U.S. Geological Survey Professional Paper 927, 52 p.
- Dunham, J. B., and Olson, E. R., 1978, Diagenetic dolomite formation related to Paleozoic paleogeography of the Cordilleran Miogeocline: *Geology*, v. 6, p. 556-559.
- Eakin, T. E., Schoff, S. L., and Cohen, Philip, 1963, Regional hydrology of a part of southern Nevada--A reconnaissance: U.S. Geological Survey Trace Elements Investigations 833, 40 p.
- Garber, M. S., and Koopman, F. C., 1968, Methods of measuring water levels in deep wells, chap. A1 of bk. 8, Instrumentation: U.S. Geological Survey Techniques of Water-Resources Investigations, 23 p.
- Greenhaus, M. R., and Zablocki, C. J., 1982, A Schlumberger resistivity survey of the Amargosa Desert, southern Nevada: U.S. Geological Survey Open-File Report 82-897, 13 p. plus appendices.
- Healey, D. L., and Miller, C. H., 1971, Gravity survey of the Amargosa Desert area of Nevada and California: U.S. Geological Survey Report USGS-474-136, 29 p. [Available only from U.S. Department of Commerce, National Technical Information Service, Springfield, Virginia 22151.]
- Hunt, C. B., Robinson, T. W., Bowles, W. A., and Washburn, A. L., 1966, Hydrologic basin, Death Valley, California: U.S. Geological Survey Professional Paper 494-B, p. B1-B138.
- Hutchinson, N. E., compiler, 1975, WATSTORE--National water data storage and retrieval system of the U.S. Geological Survey--User's guide: U.S. Geological Survey Open-File Report 75-426, 791 p.
- Lipman, P. W., Christiansen, R. L., and O'Connor, J. T., 1966, A compositionally zoned ash-flow sheet in southern Nevada: U.S. Geological Survey Professional Paper 524-F, p. F1-F47.
- Lipman, P. W., Protska, H. J., and Christiansen, R. L., 1972, Cenozoic volcanism and plate-tectonic evolution of the western United States, I--Early and middle Cenozoic: *Philosophical Transactions of the Royal Society of London, Series A*, v. 271, p. 217-248.

- Lohman, S. W., and others, 1972, Definitions of selected ground-water terms-- Revisions and conceptual refinements: U.S. Geological Survey Water-Supply Paper 1988, 21 p.
- Malmberg, G. T., and Eakin, T. E., 1962, Ground-water appraisal of Sarcobatus Flat and Oasis Valley, Nye and Esmeralda Counties, Nevada: Nevada Department of Conservation and Natural Resources Ground-Water Resources-- Reconnaissance Series Report 10, 39 p.
- Miller, G. A., 1977, Appraisal of the water resources of Death Valley, California-Nevada: U.S. Geological Survey Open-File Report 77-728, 124 p.
- Naff, R. L., 1973, Hydrogeology of the southern part of Amargosa Desert in Nevada: Reno, Nevada, University of Nevada, unpublished Masters Thesis, 207 p.
- Naff, R. L., Maxey, G. B., and Kaufmann, R. F., 1974, Interbasin ground-water flow in southern Nevada: Nevada Bureau of Mines and Geology Report 20, 28 p.
- Orkild, P. P., Byers, F. M., Jr., Hoover, D. L., and Sargent, K. A., 1968, Subsurface geology of Silent Canyon, Nevada Test Site, Nevada, *in* Eckel, E. B., ed., Studies of geology and hydrology, Nevada Test Site: Geological Society of America Memoir 110, p. 77-86.
- Pistrang, M. A., and Kunkel, Fred, 1964, A brief geologic and hydrologic reconnaissance of the Furnace Creek Wash area, Death Valley National Monument, California: U.S. Geological Survey Water-Supply Paper 1779-Y, p. Y1-Y35.
- Poole, F. G., and Sandberg, C. A., 1977, Mississippian paleogeography and tectonics of the western United States, *in* Stewart, J. H., Stevens, C. H., and Fritsche, A. E., eds., Paleozoic paleogeography of the western United States: Pacific Coast Paleogeography Symposium, 1st, Bakersfield, California, 1977, Proceedings; Bakersfield, California, Society of Economic Paleontologists and Mineralogists, Pacific Section, p. 67-85.
- Poole, F. G., Sandberg, C. A., and Boucot, A. J., 1977, Silurian and Devonian paleogeography of the western United States, *in* Stewart, J. H., Stevens, C. H., and Fritsche, A. E., eds., Paleozoic paleogeography of the western United States: Pacific Coast Paleogeography Symposium, 1st, Bakersfield,

- California, 1977, Proceedings; Bakersfield, California, Society of Economic Paleontologists and Mineralogists, Pacific Section, p. 67-85.
- Poole, F. G., Sandberg, C. A., and Boucot, A. J., 1977, Silurian and Devonian paleogeography of the western United States, *in* Stewart, J. H., Stevens, C. H., and Fritsche, A. E., eds., Paleozoic paleogeography of the western United States: Pacific Coast Paleogeography Symposium, 1st, Bakersfield, California, 1977, Proceedings: Bakersfield, California, Society of Economic Paleontologists and Mineralogists, Pacific Section, p. 39-65.
- Quiring, R. F., 1965, Annual precipitation amount as a function of elevation in Nevada south of 38½ degrees latitude: U.S. Weather Bureau of Research Statistics, 14 p.
- Rush, F. E., 1970, Regional ground-water systems in the Nevada Test Site area, Nye, Lincoln, and Clark Counties, Nevada: U.S. Geological Survey Water Resources-Reconnaissance Series Report 54, 25 p.
- Stewart, J. H., 1980, Geology of Nevada: Nevada Bureau of Mines and Geology Special Publication 4, 136 p.
- Stewart, J. H., and Carlson, J. E., 1978, Geologic map of Nevada: U.S. Geological Survey Miscellaneous Field Studies Map MF-930.
- Stewart, J. H., and Suczek, C. A., 1977, Cambrian and latest Precambrian paleogeography and tectonics in the western United States, *in* Stewart, J. H., Stevens, C. H., and Fritsche, A. E., eds., Paleozoic paleogeography of the western United States: Pacific Coast Paleogeography Symposium, 1st, Bakersfield, California, 1977, Proceedings: Bakersfield, California, Society of Economic Paleontologists and Mineralogists, Pacific Section, p. 137-155.
- Thordarson, William, and Robinson, B. P., 1971, Wells and springs in California and Nevada within 100 miles of point 37 D 15 M N., 116 D 25 M W. on Nevada Test Site: U.S. Geological Survey Report 474-85, 178 p.  
[Available from U.S. Department of Commerce, National Technical Information Service, Springfield, Virginia 22151.]
- Thordarson, William, Young, R. A., and Winograd, I. J., 1967, Records of wells and test holes in the Nevada Test Site and vicinity (through December 1966): U.S. Geological Survey Open-File Report-Trace Elements Investigations 872, 26 p.

- Walker, G. E., and Eakin, T. E., 1963, Geology and ground water of Amargosa Desert, Nevada-California: U.S. Geological Survey Ground-Water Resources-Reconnaissance Series Report 14, 45 p.
- White, A. F., 1979, Geochemistry of ground water associated with tuffaceous rocks, Oasis Valley, Nevada: U.S. Geological Survey Professional Paper 712-E, p. E1-E25.
- Winograd, I. J., 1971, Hydrogeology of ash flow tuff--A preliminary statement: Water Resources Research, v. 7, no. 4, p. 994-1006.
- Winograd, I. J., and Doty, G. C., 1980, Paleohydrology of the southern Great Basin, with special reference to water table fluctuations beneath the Nevada Test Site during the Late (?) Pleistocene: U.S. Geological Survey Open-File Report 80-569, 97 p.
- Winograd, I. J., and Friedman, Irving, 1969, Delineation of regional ground-water flow systems using deuterium, eastern Great Basin, Nevada [abs.]: Geological Society of America Abstracts with Programs, pt. 7, p. 239-240.
- \_\_\_\_\_ 1972, Deuterium as a tracer of regional ground-water flow, southern Great Basin, Nevada-California: Geological Society of America Bulletin, v. 83, no. 12, p. 3591-3708.
- Winograd, I. J., and Pearson, F. J., Jr., 1976, Major carbon 14 anomaly in a regional carbonate aquifer--Possible evidence for megascale channeling, south-central Great Basin: Water Resources Research, v. 12, no. 6, p. 1125-1143.
- Winograd, I. J., and Thordarson, William, 1968, Structural control of ground-water movement in miogeosynclinal rocks of south-central Nevada, *in* Eckel, E. B., ed., Studies of geology and hydrology, Nevada Test Site: Geological Society of America Memoir 110, p. 35-48.
- \_\_\_\_\_ 1975, Hydrogeologic and hydrochemical framework, south-central Great Basin, Nevada-California, with special reference to the Nevada Test Site: U.S. Geological Survey Professional Paper 712-C, p. C1-C126.